

Tidal analysis of borehole pressure
A tutorial

Mai-Linh DOAN and Emily E. BRODSKY
University of California, Santa Cruz
Romain PRIOUL and Claude SIGNER
Schlumberger-Doll Research

July 12, 2008

Contents

| | | |
|----------|---|-----------|
| 1 | Introduction | 3 |
| 1.1 | What can we learn from tides? | 3 |
| 1.2 | Extracting the tidal response | 4 |
| 1.3 | The structure of this document | 4 |
| 2 | The forcing: theoretical tidal strain | 5 |
| 2.1 | The tidal potential | 5 |
| 2.1.1 | Tidal forces exerted by a single planet | 5 |
| 2.1.2 | Tidal catalogs | 7 |
| 2.2 | Response of the Earth to tides | 9 |
| 2.3 | Computing theoretical tides | 10 |
| 2.3.1 | Orders of magnitude | 13 |
| 3 | Other load sources | 15 |
| 3.1 | Barometric load | 15 |
| 3.1.1 | Vented/Non-vented sensors | 15 |
| 3.1.2 | Barometric efficiency | 15 |
| 3.1.3 | Interpreting the transfer function of the borehole pressure relative to barometric pressure | 17 |
| 3.2 | Oceanic tides | 18 |
| 3.2.1 | Oceanic loading | 18 |
| 3.2.2 | Software to compute oceanic loading | 20 |
| 4 | Tidal analysis | 21 |
| 4.1 | Prerequisites | 21 |
| 4.2 | Preprocessing | 21 |
| 4.3 | Performing tidal analysis | 22 |
| 4.3.1 | The “credo of smoothness” - Tidal parameters | 22 |
| 4.3.2 | Frequency-domain analysis | 23 |
| 4.3.3 | Time-domain analysis | 24 |
| 4.3.4 | BAYTAPG | 26 |
| 4.4 | How reliable are the tidal parameters? | 27 |
| 5 | Interpreting the coefficients | 28 |
| 5.1 | Poroelastic response | 28 |
| 5.1.1 | Homogeneous poroelastic response | 28 |
| 5.1.2 | Fractured medium | 31 |

| | | |
|----------|---|-----------|
| 5.2 | Hydraulic response and permeability | 32 |
| 5.2.1 | Fluid flow to the well | 32 |
| 5.2.2 | Diffusion at the boundaries of the reservoir | 34 |
| 5.2.3 | Non uniform loading | 38 |
| 6 | Example: Change in hydraulic properties with time at the Piñon Flat Observa- | |
| | tory | 39 |
| 6.1 | Data presentation | 39 |
| 6.1.1 | Data | 39 |
| 6.1.2 | Barometric response | 39 |
| 6.1.3 | Preparation of the data | 40 |
| 6.2 | Analysis | 40 |
| 6.3 | Discussion | 42 |
| 7 | Conclusion | 45 |
| A | Glossary | 46 |
| B | ERTID | 48 |
| B.1 | Input | 48 |
| B.2 | Output file | 49 |
| C | SPOTL | 50 |
| C.1 | SPOTL: Some Programs for Ocean-Tide loading | 50 |
| C.2 | Using NLOADF | 51 |
| C.2.1 | Options | 51 |
| C.2.2 | Output | 52 |
| C.3 | Summary | 54 |
| D | BAYTAP | 55 |
| D.1 | Input | 55 |
| D.1.1 | Data file | 55 |
| D.1.2 | Parameter file | 56 |
| D.2 | Output | 58 |

Chapter 1

Introduction

1.1 What can we learn from tides?

Boreholes tapping confined reservoirs commonly exhibit periodic variations in pressure with two dominant periods: diurnal (~ 24 h) and semi-diurnal (~ 12 h). These oscillations reach 10 kPa and are easily recordable. In the continents, Earth tides induce these pressure changes, whereas oceanic boreholes are dominated by oceanic loading.

Earth tides have the immense advantage of being predictable. By comparing the actual observations and the predicted deformations, one can retrieve information about the formation surrounding the well, as depicted in figure 1.1. The purpose of this document is to explain how to make this comparison.

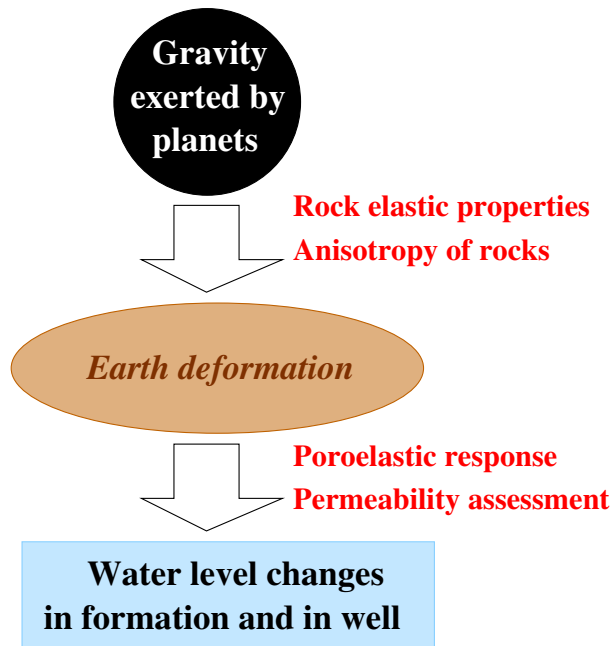


Figure 1.1: How the gravitational attraction of Moon and Sun disturbs the pressure within a well.

1.2 Extracting the tidal response

Figure 1.1 is a simplified description of the excitation of a reservoir tapped by the well. There are also some secondary effects. Figure 1.2 shows how oceanic tides and barometric variations load and deform the crust. To extract the tidal response, one must remove both effects. We will also explain how to tackle these loadings.

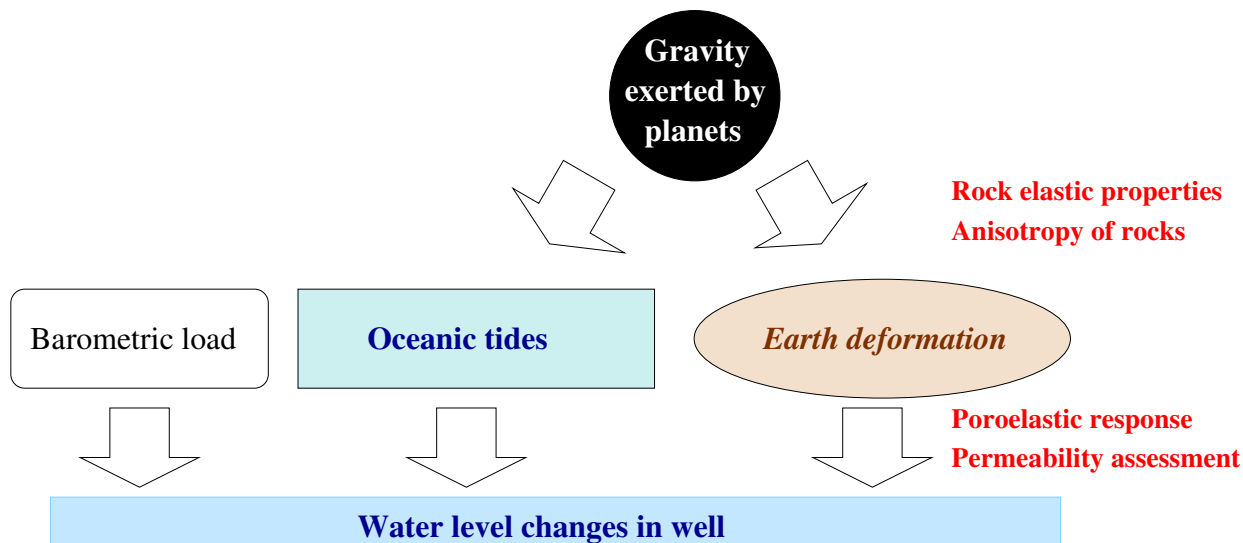


Figure 1.2: Loads other than Earth tides periodically disturb the pressure within wells.

1.3 The structure of this document

This document explains how to interpret the diurnal and semi-diurnal oscillations recorded in wells.

Before delving into the arcane of tidal analysis, we will first explain how tides deform the Earth, and hence the rocks surrounding the boreholes (**Chapter 2**). A good knowledge of Chapter 2 is not strictly necessary for an exploitation of the tidal coefficients but it helps a lot in choosing the right options among the numerous possibilities offered by tidal processing software.

A correct tidal analysis also requires the correction of oceanic and barometric load (**Chapter 3**). The oceanic load can be predicted and corrected with a specific software but the barometric load requires separate air pressure data.

Chapter 4 is the core of this document. It shows how to make a tidal analysis. We discuss one popular tidal analysis software: BAYTAP. If your purpose is just to get the values of the tidal coefficients, just read this part.

Chapter 5 shows how these tidal coefficients are related to the poroelastic and hydraulic properties of the reservoirs tapped by the well.

Chapter 6 presents an application of tidal analysis: the observation of permeability enhancement in Piñon Flat Observatory (PFO).

A glossary at the end of the document (appendix A) defines the terms that might be unfamiliar to the readers.

Chapter 2

The forcing: theoretical tidal strain

In this chapter, we will describe the theoretical Earth tides, which are the forcings of the tidal oscillations in boreholes.

We will start with a simple case, of understanding how a planet can induce diurnal and semi-diurnal changes on Earth. We introduce the notion of tidal potential, which conveniently describes the tidal forces exerted by this planet.

Next, we discuss the various phenomena which contribute to the richness of the tidal signal: the influence of other planets and the effect of the Earth ellipticity. The major tidal catalogs are presented.

The next step is to compute the deformation induced by the tidal forces. This is not a trivial step. This is a global phenomenon, relying on the mechanical equilibrium of the whole Earth. It is furthermore altered by local heterogeneities or anisotropies.

We finish this chapter by the computation of theoretical tides with the ERTID program.

2.1 The tidal potential

2.1.1 Tidal forces exerted by a single planet

A planet of mass \mathbf{M} exerts a gravitational force on a mass m distant by r . This force is equal to:

$$\vec{F} = -m \left(\frac{\mathcal{G}\mathbf{M}}{r^3} \right) \vec{r} \quad (2.1)$$

Gravitational forces are not uniform. Consider two points diametrically located on the Earth. Because of the dependence in r of equation (2.1), the forces on these points will be different: the point closer to the planet P will be more attracted by it. Tidal forces exerted by the planet P are the heterogeneity of the gravitation field created by P . Thus, tidal forces are tearing forces. The tides generated by large planets can even break apart small asteroids passing nearby (for instance, the Shoemaker-Levy comet before it crashed on Jupiter).

Let us consider a point M at the surface of Earth, of center O (figure 2.1). The tidal acceleration induced by a planet of center P is defined as:

$$\vec{g} = \mathcal{G}\mathbf{M} \left(\frac{P\vec{M}}{PM^3} - \frac{P\vec{O}}{PO^3} \right) \quad (2.2)$$

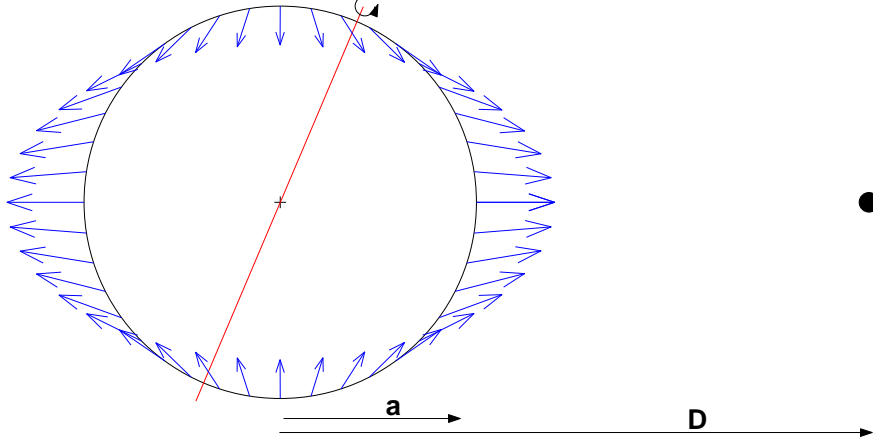


Figure 2.1: Tidal forces generated by a planet P on the Earth. Notice that the Earth axis (red line) is tilted relative to the ecliptic plane, so that the tides are not symmetric relative to the Equator.

To highlight the small dislocating effect, we removed the force exerted at the center of the Earth. Notice that strictly speaking, the resulting force is not symmetric relative to the Earth center. However, the distance PO is so large, that this asymmetry is negligible.

One likes also to define the tidal potential W so that $\vec{g} = -\vec{\nabla}W$. From equation (2.2), we have:

$$W = \mathcal{G}\mathbf{M} \left(\frac{1}{PM} - \frac{1}{PO} - \frac{OM \cos \widehat{POM}}{PO^2} \right) \quad (2.3)$$

The expression of PM is cumbersome, so equation (2.3) is rewritten in term of the Earth radius $a = OM$ and the distance separating the planet form Earth $D = PO$ by using the Legendre polynomials P_l :

$$W = \frac{\mathcal{G}\mathbf{M}}{D} \sum_{n=2}^{\infty} \left(\frac{a}{D} \right)^n P_n \left(\cos \widehat{POM} \right) = \sum_n W_n \quad (2.4)$$

As a/D is small (equal to 10^{-2} for the Moon and to 4×10^{-5} for the Sun), the sum in equation (2.4) converges rapidly. In most cases, the first term of degree 2, W_2 , is sufficient. Some very accurate catalogs can go until degree 6 (see table 2.1).

Because of the rotation of the Earth, the angle \widehat{POM} evolves, and the potential W changes. The angle \widehat{POM} is related to the latitudes λ and longitudes ϕ_M of the observation point M and of the celestial body ϕ_P via:

$$\cos \widehat{POM} = \sin(\lambda_M) \sin(\lambda_P) + \cos(\lambda_M) \cos(\lambda_P) \cos(\phi_M - \phi_P) \quad (2.5)$$

ϕ_M , the longitude of the observation point varies with time t while the Earth rotates on its axis. Within a geocentric referential (whose axes do not move with Earth; one of the axes being parallel to the Earth rotation axis), $\phi_M = \omega t$ where ω is the pulsation related to the Earth rotation of period $2\pi/\omega = T \sim 24$ h. Similarly, the position (λ_P, ϕ_P) of the celestial body is well known from astronomic observations and its trajectory with time can be computed (the Ephemeris). The quantity in equation (2.5) and thus in equation (2.4) is then easily computed.

Let's consider first W_2 the tidal potential of order 2 induced by the Moon. Because $P_2(x) = (3x^2 - 1)/2$, we get from equation (2.4):

$$W_2 = \frac{\mathcal{GM}}{2D} \left(\frac{a}{D}\right)^2 \left(3 \cos^2 \widehat{POM} - 1\right) \quad (2.6)$$

$$W_2 = \frac{\mathcal{GM}}{2D} \left(\frac{a}{D}\right)^2 \left(3 [\sin(\lambda_M) \sin(\lambda_P) + \cos(\lambda_M) \cos(\lambda_P) \cos(\omega t - \phi_P)]^2 - 1\right) \quad (2.7)$$

$$\begin{aligned} W_2 &= \frac{\mathcal{GM} a^2}{32D^3} [3 \cos(2\lambda_M) - 1] [3 \cos(2\lambda_P) - 1] \\ &+ \frac{3\mathcal{GM} a^2}{8D^3} [\sin(2\lambda_M) \sin(2\lambda_P) \cos(\omega t - \phi_P)] \\ &+ \frac{\mathcal{GM} a^2}{32D^3} [\cos^2 \lambda_M \cos^2 \lambda_P \cos(2\omega t - 2\phi_P)] \end{aligned} \quad (2.8)$$

We then get three frequencies. In inverse order of apparition in equation (2.8): the semi-diurnal wave, due to the fact that tidal forces create two symmetric bulges on figure 2.1, the diurnal wave due to the fact that the Moon is not on the equator ($\lambda_P \neq 0$) and a "constant" independent of the rotation of the Earth. But in reality, things are more complicated.

In fact, the Moon revolves also around the Earth. λ_P and ϕ_P evolve also, with a period of about 28 days. This complicates the spectrum of equation (2.8). The "constant" of equation (2.8) is in fact oscillating with a period of 14 days, giving the long period tide M_f^1 . The Moon's revolution around the Earth modulates also the $2\omega t$ and ωt oscillations in equation (2.8). This induces a triplication of the frequency $\omega/(2\pi)$, as the following trigonometric relationship shows:

$$(A + B \cos \Omega t) \cos \omega t = A \cos \omega t + B/2 [\cos((\omega - \Omega) t) + \cos((\omega + \Omega) t)] \quad (2.9)$$

Injecting equation (2.9) in equation (2.8), we get terms of the form $\cos((m\omega + l\Omega)t + \text{constant})$, where $m = 0, 1, 2$ and $l = -2, -1, 0, 1, 2$. Each term of the development is called a tidal wave.

Other phenomenon affect the movement of the Moon: the Moon orbit is not circular (ellipticity), the perigee of the Moon is drifting (as well as its obliquity, the angle between the Moon and the ecliptic plane). Even when considering a single planet, the tidal spectrum is not simple.

2.1.2 Tidal catalogs

Moreover, the Moon is not the only celestial body causing tides on Earth. Tides are exerted by all bodies from the solar system! But Moon and Sun are the main contributors to the tidal forces exerted on Earth².

The first tidal catalog is due to Doodson. Because of its historical importance, we will spend a little time describing it. Doodson considered only the Sun and the Moon as attracting bodies. At first sight, only three parameters would be needed: (1) to describe the rotation of the Earth, (2) to describe the revolution of the Moon around the Earth and (3) to describe the revolution of the Earth around the Sun. However, the orbit of the Moon around the Earth varies with time: (4) the position of its perigee and (5) its nodes. As for the revolution of the Earth around the Sun, the perihelion changes with time (6).

¹Moon fortnightly

²Venus, the next planet to exert a substantial tidal acceleration has an amplitude more than 10^4 less than the one of Sun. At the usual resolution (at best 1%) at which the tidal oscillations are recorded in wells, this is negligible, but not for gravimeter which claim a precision reaching 10^{-6} of the amplitude of the tidal acceleration.

| Authors | Waves | Bodies considered |
|------------------------|-------|-------------------------------------|
| Doodson (1921) | 377 | $n = 3$, Moon, Sun |
| Cartwright (1971,1973) | 505 | $n = 3$, Moon, Sun |
| Büllesfeld (1985) | 656 | $n = 4$ |
| Tamura (1987) | 1200 | |
| Xi (1989) | 3070 | |
| Tamura (1993) | 2060 | Venus, Jupiter |
| Roosbeck (1996) | 6499 | Planets, $n = 5$, Earth flattening |
| Hartman et al. (1995) | 12935 | Planets, $n = 6$, Earth flattening |

Table 2.1: Tidal catalogs (after [Wilhelm et al., 1997, p10])

Doodson used a set of six parameters to express the effects of the 6 phenomena. They are listed in the following table[Melchior, 1983, Harrison, 1985]:

| Phenomenon | Descriptive quantity | Period | Frequency [Hz] |
|--------------------------------------|-------------------------------------|---------------|--------------------------------|
| Earth rotation | Time angle in lunar day | 1 lunar day | $f_1 = 1.1182 \times 10^{-5}$ |
| Moon's orbit | Moon's mean longitude | 30 lunar days | $f_2 = 4.2362 \times 10^{-7}$ |
| Earth's revolution around the Sun | Sun's mean longitude | 1 year | $f_3 = 3.1689 \times 10^{-8}$ |
| Precession of Moon's perigee | Longitude of the mean perigee | 8.847 years | $f_4 = 3.5817 \times 10^{-9}$ |
| Recession of Moon's nodes | Negative longitude of the mean node | 18.613 years | $f_5 = 1.7025 \times 10^{-9}$ |
| Precession of the Earth's perihelion | Longitude of the perihelion | 20940 years | $f_6 = 1.5123 \times 10^{-12}$ |

By making a trigonometric expansion like in equation (2.7), we get a sum of trigonometric functions with arguments of the form $2\pi(n_1 f_1 + n_2 f_2 + n_3 f_3 + n_4 f_4 + n_5 f_5 + n_6 f_6)t + \phi$. The numbers $\{n_i\}$ (between -2 and 2 for a second order development) are called the Doodson numbers³. The number of possibilities is large and contributes to the complexity of the tidal spectrum (See figure 4.2). The tidal expansion gives a list of frequencies denoted by their Doodson numbers, together with an amplitude and a phase. This list is long and contains many terms of various origins and hence is called a catalog.

Since Doodson, several authors have generated several catalogs. The catalog are computed by expanding the degree of the Taylor development of equation (2.4). They also consider more attracting bodies (Venus, Mars, etc). Also the catalogs differs by their choice of ephemeris and by the consideration of secondary effects, such as the non-sphericity of the Earth. Symbolic calculus programs ease the development of large potentials, as seen in table 2.1. However, for the strain/pore pressure development, large and precise catalogs are an overkill. Increasing the number of tidal waves makes the tidal analysis computationally expensive. They reach an exceeding large precision compared to the accuracy of the theoretical strain tides, which are limited by our knowledge of the elastic properties of the Earth. This last topic is the subject of the next section.

³The initial Doodson number were n_1 and $\{(n_i + 5)\}$ for $i > 1$, to ensure that the number would be positive [Melchior, 1983]. Given the difference in order of magnitude of the considered frequencies, the Doodson numbers classed in a lexicographic order also class the tidal waves by increasing frequency.

| Name | Period [day] | Frequency [cpd] | Origin | Doodson Numbers | | | | | Typical Amplitude | | |
|-------------------------|-----------------|--------------------|----------|-----------------|----|----|----|---|-------------------------------|---------------------------------|-----|
| | | | | | | | | | Vertical Displacement [mm] | Gravity [nm/s ²] | |
| M_m | 27.554 | 0.0363 | Moon | 0 | 1 | 0 | -1 | 0 | 0 | 7 | 23 |
| M_f | 13.660 | 0.0732 | Moon | 0 | 2 | 0 | 0 | 0 | 0 | 14 | 43 |
| Q_1 | 1.1195 | 0.8933 | Moon | 1 | -2 | 0 | 1 | 0 | 0 | 19 | 59 |
| O_1 | 1.0758 | 0.9295 | Moon | 1 | -1 | 0 | 0 | 0 | 0 | 100 | 309 |
| M_1 | 1.0347 | 0.9665 | Moon | 1 | 0 | 0 | 1 | 0 | 0 | 8 | 44 |
| P_1 | 1.0027 | 0.9973 | Sun | 1 | 1 | -2 | 0 | 0 | 0 | 47 | 144 |
| S_1 | 1.0000 | 1.000 | Sun | 1 | 0 | 0 | -1 | 0 | 0 | 1 | 3 |
| K_1 | 0.9973 | 1.0027 | Moon+Sun | 1 | 1 | 0 | 0 | 0 | 0 | 141 | 434 |
| J_1 | 0.9624 | 1.0391 | Moon | 1 | 2 | 0 | -1 | 0 | 0 | 8 | 24 |
| OO_1 | 0.9294 | 1.0760 | Moon | 1 | 3 | 0 | 0 | 0 | 0 | 4 | 13 |
| $2N_2$ | 0.5377 | 1.8598 | Moon | 2 | -2 | 0 | 2 | 0 | 0 | 3 | 8 |
| N_2 | 0.5274 | 1.8961 | Moon | 2 | -1 | 0 | 1 | 0 | 0 | 21 | 64 |
| M_2 | 0.5175 | 1.9324 | Moon | 2 | 0 | 0 | 0 | 0 | 0 | 108 | 332 |
| L_2 | 0.5080 | 1.9685 | Moon | 2 | 1 | 0 | -1 | 0 | 0 | 21 | 64 |
| S_2 | 0.5000 | 2.0000 | Sun | 2 | 2 | -2 | 0 | 0 | 0 | 50 | 154 |
| K_2 | 0.4986 | 2.0056 | Moon+Sun | 2 | 2 | 0 | 0 | 0 | 0 | 14 | 42 |
| M_3 | 0.3450 | 2.8986 | Moon | 3 | 0 | 0 | 0 | 0 | 0 | 1 | 4 |

Table 2.2: Major waves for a latitude of 50° [Wilhelm et al., 1997, p22]

2.2 Response of the Earth to tides

So far, we can compute only gravitational force (or equivalently acceleration or potential). What generates the tidal variations in a well is the tidal strain. How does it appear?

The mechanical response of the Earth to tidal forces is global. Because of the long time scales of the tides, the Earth has the time to equilibrate mechanically to Earth tides. Love computed exactly the response to the Earth tides [Melchior, 1983] in the case of an homogeneous elastic Earth. He ignored any secondary effect like the Earth ellipticity, the Earth rotation and the ocean load. The displacement at the surface of the Earth is parametrized by two sets of parameters:

$$u_z = \sum_n \frac{h_n}{g} W_n \quad (2.10)$$

$$u_\theta = \sum_n \frac{l_n}{g} \frac{\partial W_n}{\partial \theta} \quad (2.11)$$

$$u_\phi = \sum_n \frac{l_n}{g} \frac{1}{\sin \theta} \frac{\partial W_n}{\partial \phi} \quad (2.12)$$

h_n are the Love numbers, l_n are called the Shida numbers. These numbers are dependent of the deep Earth structure. Numerical simulations enable to compute the Love and Shida numbers for more realistic structures of the Earth.

New estimations of the Shida and Love numbers are performed as the Earth structure is better known (as refinements to the PREM seismological model are known). This gives a variety of Love numbers to be found in the Earth tides literature. Table 2.3 shows that a variety of Love numbers have been adopted by the programs that compute the theoretical Earth tides (and also analyze

Figure 2.2: Theoretical Earth tides predicted by ETGTAB software for the moon eclipse of May 4, 2004, 20: 30UT to the north-east of Madagascar.

Figure 2.3: Predicted tidal strain in the north-south, east-west and vertical direction. The three strains do not have the same spectral content, neither they have the same phase. The tides were computed with ETGTAB

them). Given this uncertainty⁴, it is wise to consider that **the resolution of the tidal analysis of strain (and well) data cannot exceed 1%**.

This enables to compute the strain tensor:

$$\epsilon_{rr} = \frac{\partial u_r}{\partial r} = \sum_n \frac{h_n}{ga} \frac{\partial W_n}{\partial r} \quad (2.13)$$

$$\epsilon_{\theta\theta} = \frac{u_r}{r} + \frac{1}{r} \frac{\partial u_\theta}{\partial \theta} = \sum_n \frac{1}{ga} \left(h_n W_n + l_n \frac{\partial^2 W_n}{\partial \theta^2} \right) \quad (2.14)$$

$$\epsilon_{\phi\phi} = \frac{u_r}{r} + \frac{u_\theta \cot \theta}{r} + \frac{1}{r} \frac{\partial u_\theta}{\partial \theta} = \sum_n \frac{1}{ga} \left(h_n W_n + l_n \cot \theta \frac{\partial W_n}{\partial \theta} + \frac{l_n}{\sin \theta} \frac{\partial^2 W_n}{\partial \phi^2} \right) \quad (2.15)$$

Thanks to the properties of the Legendre function⁵, the total areal strain Δ_h simplifies to

$$\Delta_h = (\epsilon_{\theta\theta} + \epsilon_{\phi\phi}) = \sum_n \frac{2h - n(n+1)l}{g} \frac{W_n}{a} \quad (2.16)$$

The equation for the vertical strain ϵ_{rr} is not easy to compute⁶, so we rather use the relationship $\epsilon_{rr} = -\frac{\nu}{1-\nu} \Delta_h$, derived from the free surface boundary condition.

The volumetric strain Δ is then

$$\Delta = \frac{1-2\nu}{1-\nu} \Delta_h = \sum_n \frac{1-2\nu}{1-\nu} \frac{2h - n(n+1)l}{g} \frac{W_n}{a} \quad (2.17)$$

Notice that the volumetric strain is negative relative to the tidal vertical displacement! The inner compliant layer pushes the more rigid crust. As when a balloon is inflated, the shell is expanding. The areal strain dominates the volumetric strain, and gives its sign. Figure 2.2 shows this phenomenon.

Note that the phase of strain, tilt and gravity are not the same (figure 2.3), except in exceptional case like in figure 2.2. This creates problems when demonstrating a correlation between tides and earthquake occurrence. The component to be tested must be rigorously specified (nature and direction).

A last problem stains the prediction of the theoretical strains. The actual strains are very dependent on the presence of cavities [Harrison, 1976]. They are also very dependent of the present of anisotropy [Bower, 1983].

⁴Which is intrinsic to the fact that the Love numbers presuppose a layered Earth, and thus do not account for the heterogeneity of the surface

⁵They are defined as the solution of the differential equation: $(1-x^2) \frac{\partial^2 P_n(x)}{\partial x^2} - 2x \frac{\partial P_n(x)}{\partial x} = -n(n+1)P_n(x)$.

⁶They involve the gradient $\frac{\partial h_n}{\partial r}$.

2.3 Computing theoretical tides

Several programs compute the theoretical strain tides. Most programs are written by scientists for scientists and no license are provided with the program by default. Often, the authors have published a short description of their program. Their publications should be cited when publishing a work performed with their program. We indicate when a specific license applies to a program. Here is a set of popular programs⁷:

- **ETGTAB** by H.G. Wenzel. Its output is in the “international standard format for the storage and exchange of high resolution earth tide data” (in short, the ETERNA format)
- The **PREDICT** program of the ETERNA tidal analysis software is written by the same author and gives the same results.
- The **MT80W** program provided by ICET. The program is an old-fashioned Fortran program with fixed formatting of the input.
- The **ERTID** program of the PIASD tidal analysis software⁸, adapted by D.C. Agnew from a program written initially by D.E. Cartwright. It is also included with the SPOTL software for computing the oceanic tides.

To limit the number of programs to use, we will focus on the ERTID software, which is described in detail in appendix B.

We will here focus on the similarities and dissimilarities of these software.

All programs require essential input:

- The position of the station: latitude, longitude and elevation (this last parameter is less critical).
- The time span of the output (UT time).

You cannot do any relevant tidal analysis without knowing position and time.

Some other choices are optional:

- The tidal catalog. Programs which use a catalog by default (PIASD and MT80W) use the Cartwright catalog.
- The gravity at the considered point. If not specified, the model use some reference model (GRS80 for ETGTAB, for ERTID).
- The component needed. We are interested in areal strain (or volumic strain) but some program do not provide it directly (eg. ERTID). To retrieve it, you just need to compute the horizontal strain in two perpendicular directions and sum up the quantities.

In some program, there is an option to provide the tidal parameters

2.3.1 Orders of magnitude

As shown on figure 2.2, the amplitude of the tidal volumic strain is about $50 \text{ nstrain} = 5 \times 10^{-8}$. With a typical Skempton coefficient of 0.8 and a bulk modulus of 20 GPa, the expected pressure tides are about 800 Pa. Thus, a resolution of a least 200 Pa is necessary for the pressure data.

⁷There are other tidal software. For instance, T_TIDE runs under Matlab, but this program is designed for oceanographic study and does not compute any strain

⁸This programs has a license which states it can be used freely. See the `copying` file provided with the program for full license.

| Software | h_2 | l_2 | k_2 |
|------------------------------|--------|--------|--------|
| [Wilhelm et al., 1997, p.46] | 0.6033 | 0.0838 | 0.2980 |
| PREM | 0.6032 | 0.0839 | 0.2990 |
| Gutenberg-Bullen | 0.6114 | 0.8832 | 0.3040 |
| MT80W (MOLODENSKY model) | 0.6206 | 0.0904 | |
| ETGTAB/ETERNA | 0.6165 | 0.0840 | 0.3068 |
| PIASD | 0.6114 | 0.0832 | 0.304 |
| BAYTAP | 0.606 | 0.0840 | 0.299 |

Table 2.3: Love parameters used by various tidal prediction software. Notice that the variations exceed 1%.

Chapter 3

Other load sources

3.1 Barometric load

3.1.1 Vented/Non-vented sensors

Most of the fluid level sensors are indeed pressure transducers. Hence, they record both the weight of the fluid column and the atmospheric pressure.

Some fluid level sensors are vented: a tube connects the sensor to the open air so that the sensor can also record the atmospheric pressure. In that case, the sensor subtracts the atmospheric pressure to the total pressure and gives a direct value of the fluid level.

Vented sensors are more expensive than non-vented one. They are also more difficult to use because of the tube connecting the sensor to the open air make the vented cable more voluminous and fragile. Hence, they are usually used only when needed, that is exclusively in open wells.

3.1.2 Barometric efficiency

Yet, even in the case of a vented sensor, like the one displayed in the top graph of figure 3.1, the data are correlated to changes in barometric pressure. Atmospheric pressure applies a load on the surface of the Earth. Hence, it deforms the matrix of the reservoir, like the Earth tides do. And it changes the pressure, such as the Earth tides do. Supposing that the response is still undrained, the change in pressure in a porous medium is:

$$p = \gamma p_{atm} = \frac{B(1 + \nu_u)}{3(1 - \nu_u)} p_{atm} \quad (3.1)$$

where B is the Skempton coefficient, ν_u is the undrained Poisson ration and γ is defined as the barometric efficiency. Typical values of barometric efficiency are between 0.3 and 0.8. As for Earth tides, fluid flow may induce frequency dependent response and greatly complicate the removal of atmospheric pressure before tidal analysis.

For barometric loading, we have to distinguish the cases of open wells and closed wells (table 3.1).

Most of the tidal analysis programs neglect frequency dependence in the barometric correction. The reason is that the atmospheric pressure is still a second-order effect compared to the tidal variations. On the bottom graph of figure 3.1, the atmospheric pressure exhibits 100 Pa of diurnal and semi-diurnal variations, mainly due to thermal expansion, but also due to the forcing of the atmosphere by tidal forces. As the Skempton coefficient is around $B \sim 0.8$, the barometric contribution is about 80 Pa, in a closed well (γ) or an open well with a vented sensor ($1 - \gamma$) or non-vented sensor

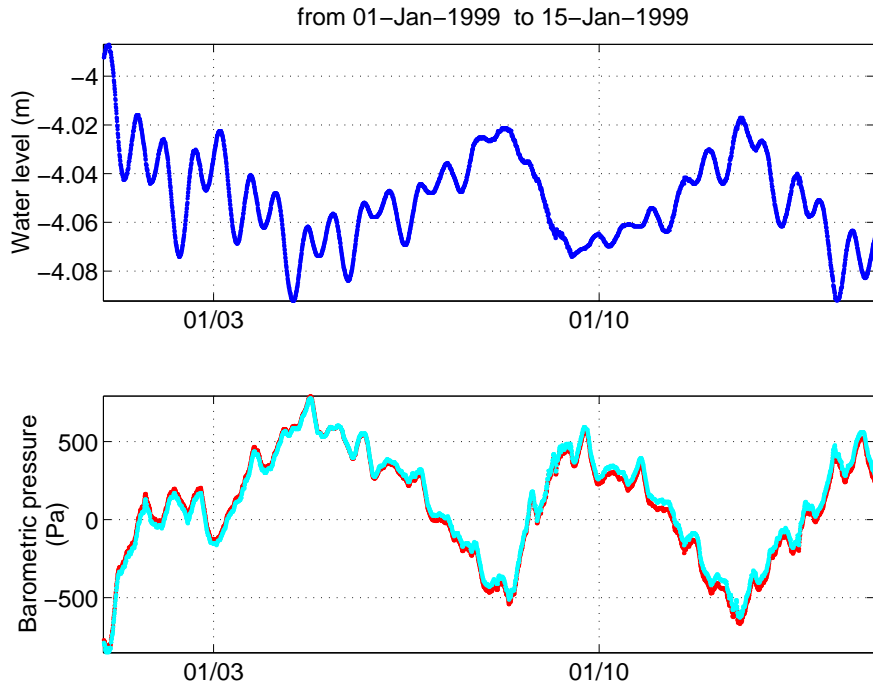


Figure 3.1: Water level recorded in well CIB of the Piñon Flat Observatory (top) and atmospheric pressure on the site during the first 15 days of 1999. The two data are correlated and exhibit diurnal and semi-diurnal oscillations.

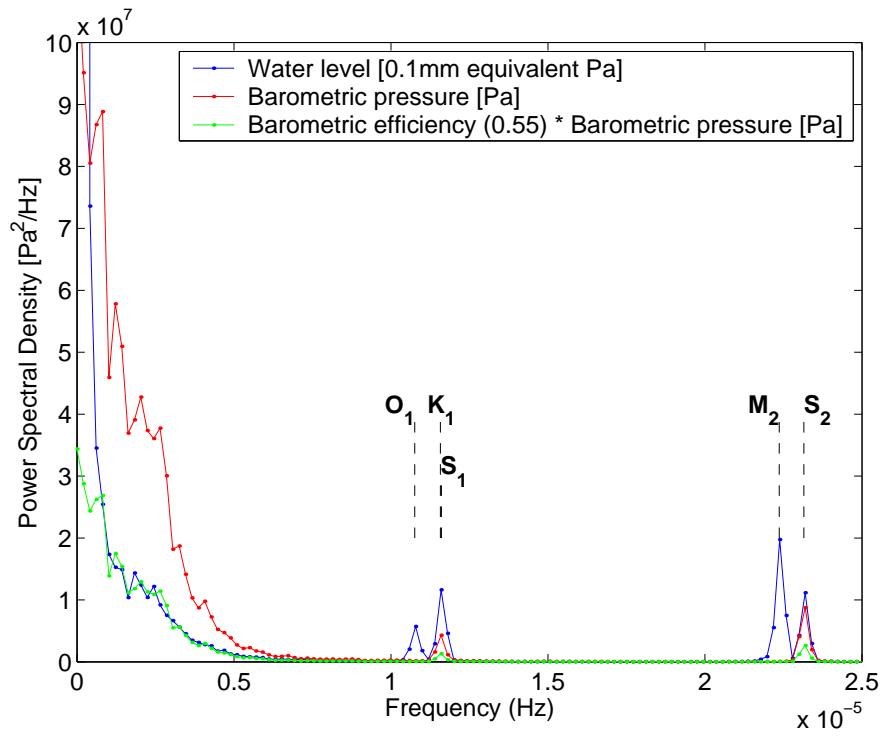


Figure 3.2: Spectrum of the data presented in figure 3.1, computed from the data from 1990 to 1999.

| Recording configuration | Sealed well | Open well | |
|----------------------------------|-----------------------|------------------------------|-----------------------|
| | Pressure data | Vented sensor | Non-vented sensor |
| Response to atmospheric pressure | γ (> 0) | $-(1 - \gamma)$ (< 0) | γ (> 0) |

Table 3.1: Theoretical sensitivity of the pressure data depending on the configuration of the recording. γ is the barometric efficiency, defined in equation (3.1).

γ . The pressure change in figure 3.1 is of about 800 Pa, so that the pressure changes typically equal about 10% of the tides in the well.

A contribution of 10% may seem important, but the study of the spectrum of figure 3.2 provides a basis for a bit more optimism. The variations of pressure are modulated by temperature, that changes on a daily basis with the sunlight. The pressure spectrum is thus related to the Sun, and has its peaks in the S_1 , S_2 , S_3 constituents. In particular, the thermal effect spoils the K_1 coefficient. The spectrum of the Earth tides is much richer. The tidal constituents O_1 and M_2 have large amplitudes and less affected by barometric effect, and are the favorite constituents used in the interpretation of tidal analysis.

The quality of the tidal analysis is greatly enhanced if you take into account the changes in barometric pressure. Most popular tidal analysis programs enable to invert jointly the dependence of the data on Earth tides and atmospheric pressure. Moreover, you gain more information about the medium by exploiting also the barometric data. An example in figure 3.2 shows that the fluctuation of the pressure between 2 days and 15 days is due to the barometric loading¹. We get a barometric efficiency of 0.55, which provides information on the medium through equation (3.1).

3.1.3 Interpreting the transfer function of the borehole pressure relative to barometric pressure

Atmospheric pressure loads the formation whose hydraulic head is measured over a wide range of frequencies. This provides interesting information on the spectral response of the well to a known loading.

The response of the reservoir to barometric loading indicates in which regime the well is (See chapter 5 for more details). For instance, if the amplitude is at a plateau, then no hydraulic effect spoils the data, and the tidal response can be used to assess the poroelastic coefficient of the medium with confidence.

As shown in section 5.2, the transfer function estimated from the barometric loading should be estimated on the equivalent fluid level data. That means that you:

- directly compute the transfer function relative to the atmospheric pressure directly from the raw data if you work with the data acquired in a closed well or by a non-vented sensor in an open well.
- compute the transfer function relative to the atmospheric pressure directly from the raw data *subtracted from the barometric pressure* if you work with the data acquired with a vented sensor in an open well.

An example of the utilization of the spectral response to barometric loading is given in Chapter 6.

¹Beyond, rain effect and yearly hydraulic cycle have to be taken into account.

3.2 Oceanic tides

Although oceanic tides are generated by the same gravitational forces than Earth tides, the ability of the ocean to redistribute mass gives to oceanic tides their own dynamics. The oceanic tides have therefore the same spectrum than Earth tides but different amplitude and phase. To estimate the effect of oceanic load, either actual local measurements or global models are used.

3.2.1 Oceanic loading

Order of magnitude

Every point of the ocean where the ocean elevation changes by dh exerts a load $\rho_f g dh$. The effect of each load on the observation point is computed through a Green function. To estimate the effect of oceanic loading, we need (1) a good description of the oceanic tides and (2) a good knowledge of the elastic structure of the Earth.

Global models have been greatly enhanced with the data provided by the satellites TOPEX/POSEIDON and JASON (figure 3.3). Ocean level changes can be several meter large. This change of elevation (1) loads the Earth, like the barometric pressure does and (2) exerts a gravitational force. In the case of strain, only the first effect is significant.

To get an order of magnitude, we can use the Green Function for stress associated to a point load F at the surface of a homogeneous half-space (the Boussinesq solution)[Craig, 1987]:

$$p = B \frac{(\sigma_{zz} + \sigma_{rr} + \sigma_{\theta\theta})}{3} = B \frac{z(1 + \nu_u)}{\pi R^3} \quad (3.2)$$

One sees that the oceanic load decays very fast as $z/R^3 \sim 1/r^2$ (for gravity, it is only $1/r$, and gravicists bother much more about oceanic tides). One advantage at considering strain (and pressure) is that the oceanic loading decays faster than for gravity. However, the contribution is sufficiently large to induce a 7° lag in the Piñon Flat Observatory 100 km from the seashore.

Notice how heterogeneous is the amplitude near the coasts in figure 3.3. This is due to local hydrodynamic resonances. Hence, **if the well is near the seashore or under water, it is highly recommended to get tide gauge data**. For instance, the AIG10 well of the Corinth Rift Laboratory exhibits a strong sensitivity to oceanic tides. As it is located only 500 m from the seashore, the oceanic contribution reaches about 50% of the total oscillations. In oceanic processing of tides data, the tides are completely dominated by the oceanic loading and the Earth tides are ignored.

Therefore to take into account the ocean loading, we need:

- an oceanic model describing the tidal variation near the ocean. Modeling this is very complicated, but new satellite observation provides precise ($0.5^\circ \times 0.5^\circ$) semi-empirical description of the oceanic tides. Note that local tides are predominant and should be modeled with care. If the observation point is near the seashore, it is advised to dispose of precise local tidal data, as provided by tide gauges.
- a Green function model. This depends on the elastic parameters of the Earth chosen.

All contributions are then summed for all the components of interest.

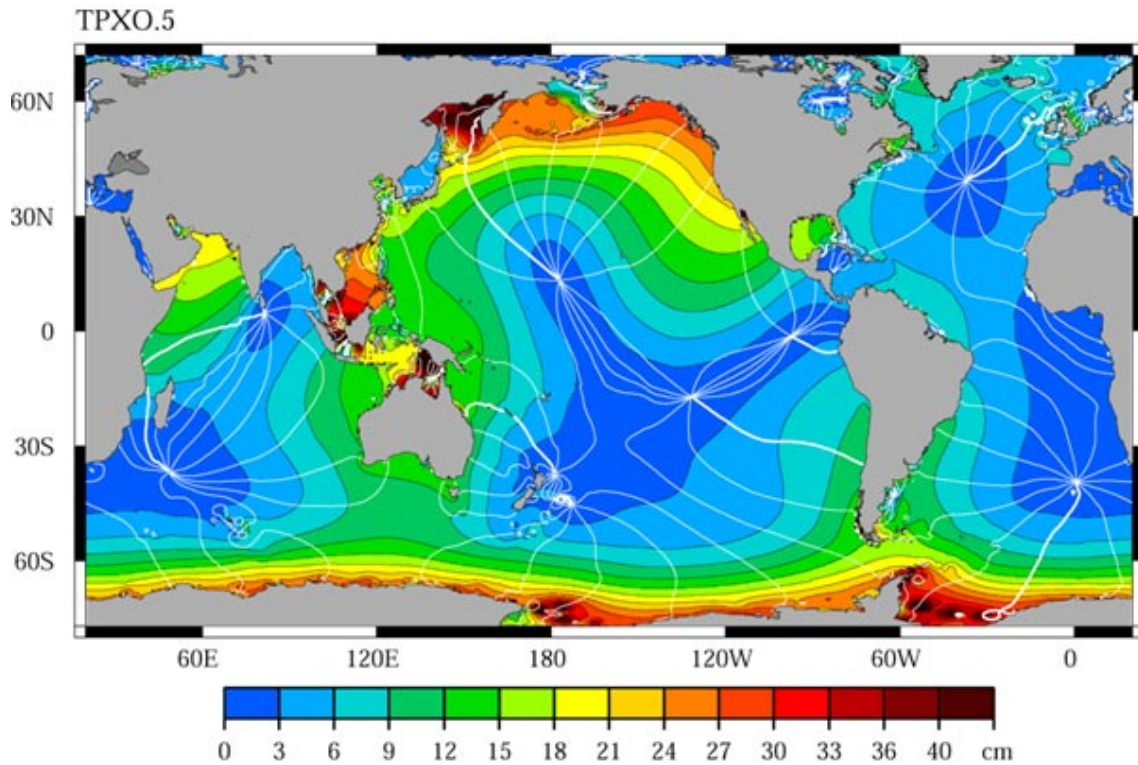
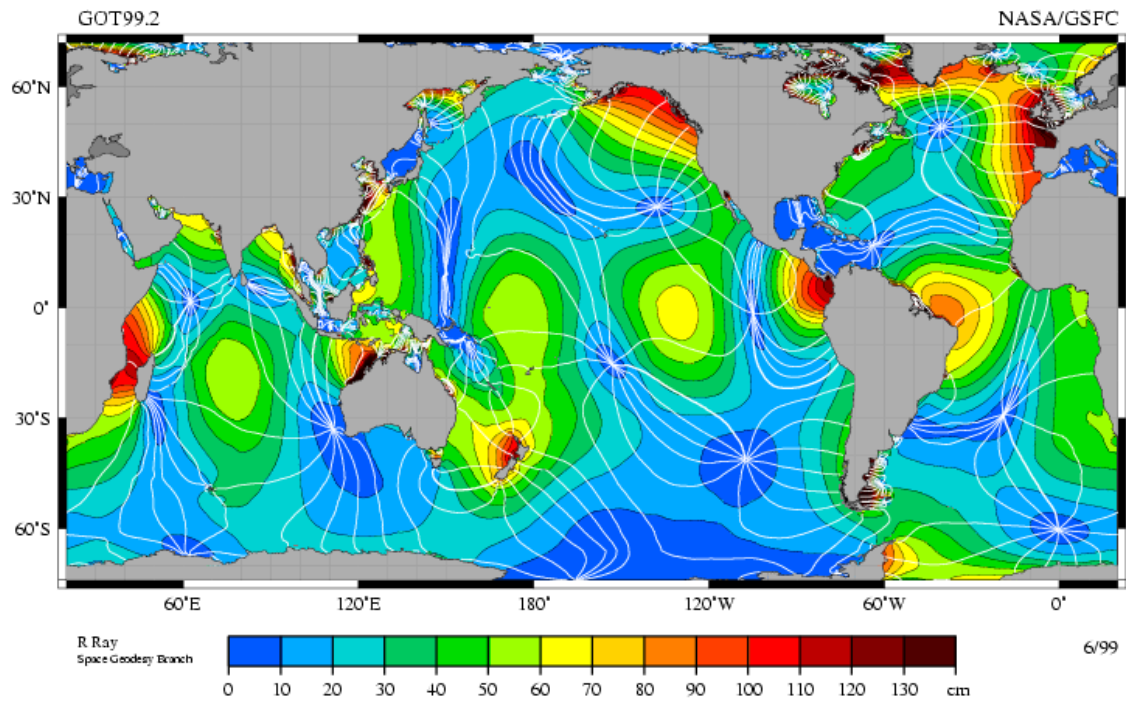


Figure 3.3: Tidal amplitude of M_2 (top) and O_1 (bottom) constituents of oceanic tides in cm (derived from the data of TOPEX/POSEIDON [Ray, 1999]). The white lines show the isophase lines. The M_2 image is retrieved from http://svs.gsfc.nasa.gov/stories/topex/images/TidalPatterns_hires.tif, the bottom image from http://www-aviso.cnes.fr:8090/HTML/information/publication/news/news8/ray_fr.html

3.2.2 Software to compute oceanic loading

Some institutions offer services to compute oceanic load coefficients for a given site:

- Chalmers University, Sweden: <http://www.oso.chalmers.se/~loading/index.html>
- Bern, Switzerland: <ftp://ftp.unibe.ch/aiub/bswmail/bswmail.0134>

They may be convenient to use, but the precise behavior of the programs are not tested here.

There are ocean loading computation programs you can install on your computer²:

- GOTIC2 National Astronomical Observatory, Mizusawa, Japan. This program is focused on Japan.
- SPOTL D.C. Agnew, Scripps Institute of Oceanography, La Jolla, California (See appendix C). Refinement of oceanic models are provided for the seas around the USA.

²Most programs are written by scientists for scientists and no license are provided with the program by default. Often, the authors have published a short description of their program. Their publications should be cited when publishing a work performed with their program. We indicate when a specific license applies to a program.

Chapter 4

Tidal analysis

Performing a tidal analysis consists in the comparison of the tidal oscillations observed relative to the theoretical Earth tides (figure 1.1).

Before that, it is useful to preprocess the data to clean it from spikes and steps. Then we compute the response of the signal relative to the tidal band. We will present one widespread program of tidal analysis: BAYTAP.

4.1 Prerequisites

To summarize the two previous chapters, here are the minimum data that are needed to perform a successful tidal inversion:

- **Data.** The duration of the data necessary depends on the precision of the tidal analysis. A minimal duration is 2 days, to get separate semi-diurnal and diurnal tide and get some rough estimate of the tidal analysis. At least 15 days are necessary to separate the 2 major sub-bands of the diurnal and semi-diurnal tides. A resolution of at least 200 Pa is necessary
- **Exact UT time and geographical location of the site.** To estimate the theoretical Earth tides.
- **The barometric pressure.** To remove this important contribution on fluid level and greatly improve the analysis.
- **Tide gauge data.** Useful for wells located very near the seashore or underwater.

4.2 Preprocessing

- Is the pressure sensor absolute or relative (to barometric pressure, so that it measures true fluid level)? To check it, compare barometric and borehole pressure fluctuations (table 3.1).
 - In an open well: if they have a positive correlation, the pressure sensor is absolute. If they have a negative correlation, the pressure sensor is relative.
 - In a closed well: the pressure sensor is absolute (there is no need to use a more expensive vented sensor in a closed well). It should have the same sign as the pressure oscillation.

Notice that in all case, the tidal signal is altered by barometric loading. Independent barometric data are necessary to clean the data from barometric loading.

- You may remove the barometric pressure or let the software do it for you (with all its limitation).
- Is the ocean load negligible? If you are located below or near sea water, the load is not negligible and dominated by local effects. You then need some tide gauge data, as global models are often too poor to predict it. Even far from the seashore, the effect of the ocean cannot be neglected. It can be small ($\sim 7^\circ$ phase in PFO, about 200 km from the seashore) but an estimation with a software like SPOTL (appendix C) for oceanic load prediction is advisable.
- Are there steps in the data? Are there spikes or transitory oscillations (earthquakes)? It is better to remove them manually. This can be done with Matlab or with the preprocessing functionalities provided by some programs. This is by far the most boring part of the analysis. If there are not so many and the data span is large, you can ignore these steps, but this will increase the error of your tidal analysis.
- Are there missing data? As most of the programs use least square inversion on time series, this is not important. If you use your own spectral method, the gaps need to be filled either by linear interpolation, or by synthetic tides. If the ratio of gaps over recording duration is large, this could result in large errors.

4.3 Performing tidal analysis

4.3.1 The “credo of smoothness” - Tidal parameters

Earth tides have a rich spectrum with different components. The response is the sum of all the frequencies of a catalog:

$$y_{th} = \sum_{k \in waves} a_k e^{i\omega_k t} \quad (4.1)$$

where a_k are complex coefficients.

The response of the well is given by a series

$$y_{resp} = \sum_{k \in waves} h_k a_k e^{i\omega_k t} \quad (4.2)$$

Performing a tidal analysis consists in retrieving the complex coefficients h_k (amplitude and phase) for each frequency. Given the number of waves listed in Tab 2.1 (at least 370), the inversion of equation (4.2) is unstable.

The strategy is to assume that the coefficients h_k will be the same for frequencies ω_k close to each other. This is the “credo of smoothness”¹. The frequencies are gathered in groups g of frequencies for which the coefficient h_k are uniform. Equation (4.2) is simplified into

$$y_{resp} = \sum_{g \in groups} h_g \sum_{k \in wave\ g} a_k e^{i\omega_k t} \quad (4.3)$$

There is only one complex coefficient per packet h_g . An example of gathering is shown in figure 4.2, where the number of packet is chosen in function of the length of the tidal data. The variable h_g is a tidal parameter, that is the quantity to be determined in tidal analysis.

¹Expression borrowed from Duncan Agnew

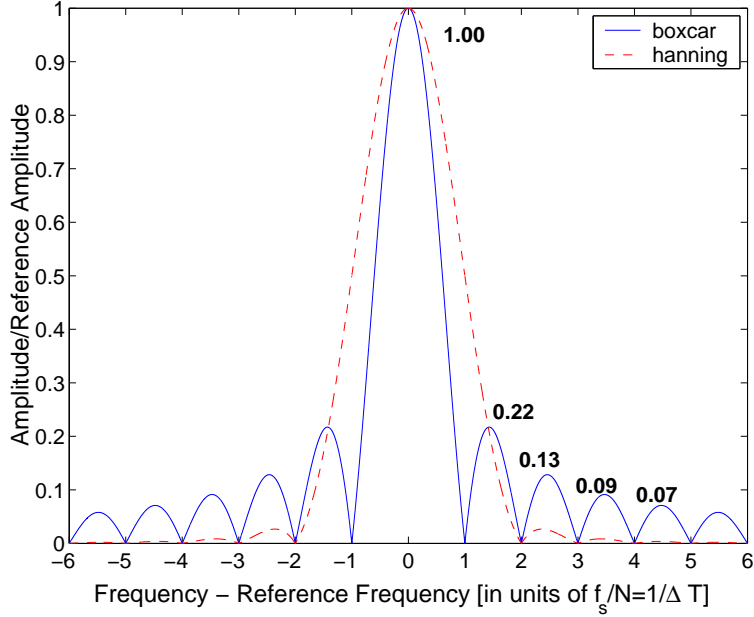


Figure 4.1: Spectral leakage induced by the finite duration of the data. Infinite length data would give a Dirac spike centered on the frequency considered (at 0 in this graph). But the finite duration of the data ΔT spreads this peak and causes several rebounds which decay very slowly. Windowing (for instance, the Hanning window $(1 - \cos(\frac{2\pi t}{\Delta T}))/2$) reduces the secondary bumps at the expense of the wider central peak.

4.3.2 Frequency-domain analysis

Performing a tidal analysis in the frequency domain deals directly with equation (4.2). It consists in comparing the Discrete Fourier Transform of the data with that of the theoretical Earth tides, preliminarily computed with one of the programs of chapter 2.

There is a criterion specifying beyond which duration you can begin to resolve a doublet of frequencies: the Rayleigh criterion. It requires that the length of the analyzed data exceeds $1/(f_{K1} - f_{O1}) = 13.6$ days and $1/(f_{S2} - f_{M2}) = 14.8$ days.

Moreover, for spectral analysis the acquisition of data over a limited period of time artificially spreads the frequency band corresponding to the tidal constituents. The secondary peaks may be especially damaging. Windowing helps to reduce the spectral leakage but widens the central peak of the leakage (figure 4.1). Therefore, for frequency domain analysis we recommend at least 28 days of data.

Reducing the spectral leakage is the first conditions for a successful tidal analysis of a tidal constituent of frequency f_0 . Another condition is to get one of the frequency of the Discrete Fourier Transform $n/\Delta T$ as close as possible to f_0 . This is an arithmetic problem, which is very dependent of the data duration ΔT . By using data of high sampling frequency f_s , one may adjust more easily the duration Δ to fulfill these two conditions. For instance, the DFT method gives reasonable results for M_2 tide in the Piñon Flat Observatory case [Elkhoury et al., 2006], because of the high-sampling rate (5 minutes).

Time-domain analysis is much widespread as it better takes into account the preexisting knowledge of tidal frequencies. All the major tidal analysis software operate in the time domain.

4.3.3 Time-domain analysis

Time domain analysis involves more than the tidal parameters $h_g = H_g e^{i\phi_g}$:

$$y_{resp} = \sum_{g \in groups} H_g \sum_{k \in waves\ g} (A_k \cos(\omega_k t + \phi_g) + B_k \sin(\omega_k t + \phi_g)) \quad (4.4)$$

+ *secondary loadings* + *trend* + *noise*

In most of the program, the influence of the barometric pressure p_{atm} (and other supplementary data as temperature or tide gauge) is reduced to the frequency-independent function $\gamma \times p_{atm}$. The program will perform a least-squares inversion to provide automatically the barometric efficiency γ . If the frequency-independent model is not appropriate, barometric pressure has to be removed by hand. BAYTAP avoids this issue by enabling a response with memory (involving not only the pressure at time t but also at time $t - 1$).

The definition of the trend depends also on the program. Some programs use interval-wide approximation. For instance, they involve the fit of long-term trend by Chebyshev polynomials (ETERNA). This method has the drawback that the fit changes if more data are added. Some prefer to use a spline interpolation, which depends only on the local properties of the trend. High-pass filtering is possible in ETERNA but this option is not very popular, since there are some risks to altering the tidal frequencies if the filter is poorly designed.

There are several tidal analysis software packages available. They differ by the tidal catalog they use, by the way they group the tidal components, by the way they process auxiliary channels, by their method of inversion. Here are the major ones²:

- ETERNA33 Runs under DOS. Fortran Code source are now available from the Global Geodynamic Project. <http://www.eas.slu.edu/GGP/ETERNA/>
Least square inversion. Vast choice of catalogs. Auxiliary channels removed by least-square inversion. Manual selection of tidal wave packets.
- BAYTAPG Fortran code source available from <http://ggpjapan.miz.nao.ac.jp/baytap/uncompress/>
Parametric inversion. Tamura or Cartwright catalogs used. Automatic selection of waves packet.
- PIASD Fortran and C code source available³. Written for UNIX. Code source available by <http://igppweb.ucsd.edu/~agnew/piasdmain.html>.
Least square inversion. Cartwright catalog. Auxiliary channel have to be preliminary removed (extensive preprocessing abilities are given with the program).

In this tutorial, we will focus on BAYTAP, which is simpler to use and easier to compile.

²Most programs are written by scientists for scientists and no license are provided with the program by default. Often, the authors have published a short description of their program. Their publications should be cited when publishing a work performed with their program. We indicate when a specific license applies to a program.

³This programs has a license which states it can be used freely. See the `copying` file provided with the program for full license.

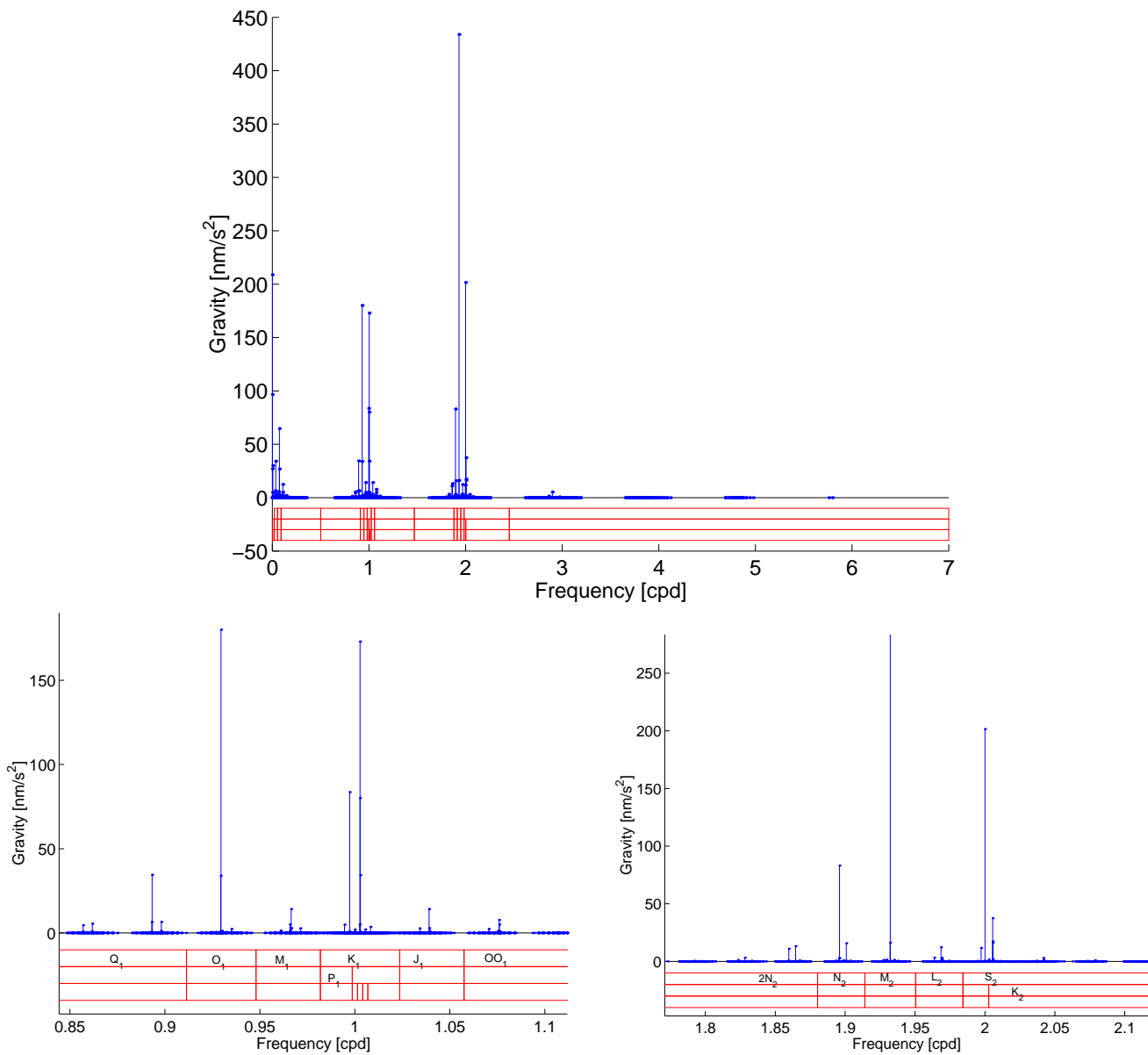


Figure 4.2: (Top) Tidal spectra of earth tides, as computed from Hartmann and Wenzel [1995]’s catalog. At the bottom of the graph, we indicate the boundaries of the wave packet suggested by the manual of ETERNA. The name of the packet is the name of its preeminent component. (Bottom left) Close up on the diurnal components. (Bottom right) Close up on the semi-diurnal components.

4.3.4 BAYTAPG

BAYTAP-G (Bayesian Tidal Analysis Program - Grouping Model) is a widespread tidal analysis program ⁴. It relies on a Bayesian model of analysis⁵, which tries to fit the data with additional constraints on the parameters.

Bayesian inversion

The program approximates the observed data y_i as:

$$y_i = \sum_g \sum_{m=0}^{N_g} (A_m C_{mi} + B_m S_{mi}) + d_i + \sum_{k=0}^K b_k x_{i-k\Delta} + h z_i + \epsilon \quad (4.5)$$

In order of appearance in equation 4.5, we recognize:

- the tidal part, in the double sum. The double sum reflects the grouping. Each coefficient is expressed as a sum of cosines C_{mi} and sines S_{mi} . The tidal analysis consists in getting the coefficients A_m and B_m .
- a long term trend d_i .
- the response to external loading. Time memory is possible (this is an improvement relative to the instantaneous model of ETERNA)
- Steps in the data can be also modeled, with a Heaviside step function. The coefficient z_i is null when no step occurs or gives the amplitude of the step is a step occurs.
- Some noise ϵ .

To estimate the quality of the fit, one considers the matching between the data and the model

$$criterion = \sum_i \|y_i - \sum_g \sum_{m=0}^{N_g} (A_m C_{mi} + B_m S_{mi}) - d_i - \sum_{ki} b_k x_{i-k} - h z_i\|^2 \quad (4.6)$$

as well as some constraints on the parameters. This is the Akaike contribution⁶.

The two constraints added are

- the smoothness of the trend by adding the term $D^2 \sum_i \|d_i - 2d_{i-1} + d_{i-2}\|^2$. If D is large, the trend is constrained to be linear and smooth. If D is small, the trend is authorized to be strongly bent to fit better the data.

⁴It is the one used as the demonstration of processing of UNAVCO strainmeter data <http://www.unavco.org:8080/cws/straindata/Notes%20from%202005%20class/>.

⁵That is an inversion performed within the framework of probabilistic theory. Thomas Bayes formulated the formula central to the inversion of the conditional probability of the parameters knowing the data and its uncertainty to the conditional probability of the knowing the parameters and its uncertainty, and vice-versa.

⁶One popular constraints is the number of parameters, which has become almost synonym to "Akaike criterion". But the Akaike contribution is to put some *general* constraints on the parameter in addition to the matching of the data and the model.

- The smoothness of the response to the Earth tides. The quantity $W^2 \sum_m \|(A_m - A_{m-1})^2 + (B_m - B_{m-1})^2\|$ is added to the residual estimate. If W is large, the response is imposed to be similar for close tidal frequencies⁷. This stabilizes the analysis, even if the number of groups of tidal constituents is large⁸.

The *ABIC* (Akaike’s Bayesian Information Criterion) is then:

$$\begin{aligned}
 ABIC = & \sum_i \|y_i - \sum_g \sum_{m=0}^{N_g} A_m C_{mi} + B_m S_{mi} - d_i - \sum_{ki} b_k x_{i-k} - h z_i\|^2 \\
 & + D^2 \sum_i \|d_i - 2d_{i-1} + d_{i-2}\|^2 + W^2 \sum_m \|(A_m - A_{m-1})^2 + (B_m - B_{m-1})^2\|
 \end{aligned} \tag{4.7}$$

Other features of the program

By default, the program selects the groups for the inversion, based on the length of the data. Only the Cartwright and al. and the Tamura catalogs are available.

It is possible to run the program several times on different subsets of the data by setting the *SPAN* and *SHIFT* option. This is very convenient to get time evolution of tidal parameters.

It can compute reference tides for gravity, tilts and azimuthal strains. But not directly for areal and volumetric strain. According to equations (2.16) and (2.17), they are directly proportional to the potential W . One can use the component $W/(ga)$ corresponding to the selection *KIND=7*. But one has one manually have to “calibrate” the value by getting the right Love numbers and elastic parameters.

More details on the practical use of the program are presented in appendix D.

4.4 How reliable are the tidal parameters?

Some tidal components are more reliable than others. Three criteria are to be taken into account:

- The amplitude of the tidal component.
- Check that the duration of the data analyzed exceeds several times the inverse of the difference between the frequencies of the waves to be investigated.
- The absence of another phenomena. Avoid S_2 which has the same frequency than thermally induced atmospheric tides (and thermal oscillations also if your sensor is temperature dependent). Avoid K_1 which is disturbed by resonances induced by the free core nutation and by barometric loading (figure 3.2).

For these reasons, the two canonical components for the semi-diurnal and diurnal tides are M_2 and O_1 .

Once you have the parameters, you can use them to derive information about the reservoir tapped by the well. This is the subject of the next chapter.

⁷This might not be true for the diurnal frequencies, affected by Free Core Nutation, a resonance of the Earth structure at near diurnal frequency. There is a special option *IFCR* to take this into account.

⁸This constraint has the disadvantage to spread the error on the tidal constituents of small amplitude onto the tidal constituents of large amplitude. It is nice if you want to get the shape of the response, less if you want only the M_2 constituent.

Chapter 5

Interpreting the coefficients

In chapters 2 and 3, we have briefly showed how the tidal strain induces pressure changes in a well. This process occurs in two phases: (1) the poroelastic phase, in which the tidal strain induces change a pressure in the equilibrium and (2) the hydraulic phase in which the change in pressure in the medium induces a change in pressure in the well. This is expressed in figure 5.1.

In this chapter, we gather the equations describing these processes already presented in a scattered version in the previous chapters. After a short description of the poroelastic theory, we will see how to interpret the tidal parameters.

5.1 Poroelastic response

5.1.1 Homogeneous poroelastic response

Minimal coefficients necessary to characterize a poroelastic medium

A pure elastic medium is characterized by two elastic coefficients¹. But the state of a poroelastic homogeneous medium is also dependent on two other quantities than the strain and the stress: its fluid content and the pressure of this fluid [Wang, 2000]. Hence the mechanical response of a porous medium is characterized by two more constants describing the properties of the pores filled with fluid. Several parameters are used for this purpose:

- Undrained build-up coefficients. The most common one is the Skempton coefficient:

$$B = \left. \frac{\partial p}{\partial \sigma} \right|_{undrained, \text{ constant volume}} \quad (5.1)$$

¹the two Lamé coefficients λ and μ , or the bulk modulus K and the Poisson ratio ν , or the Young modulus E and the Poisson ratio ν , or the velocities of the P and S waves. You can switch without ambiguity from one set of parameters to another.

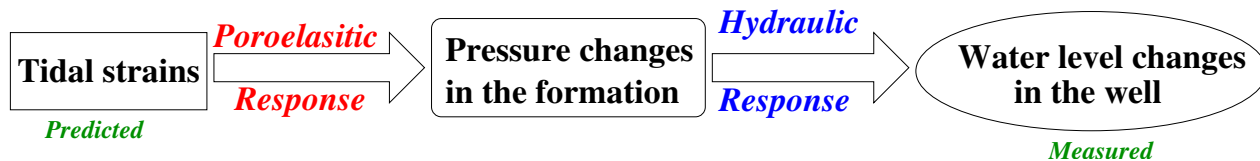


Figure 5.1: How the tidal strains are expressed as pressure changes.

- Specific storages. They describes the *ability of the formation to store fluid*. They have the form:

$$S_{boundary\ conditions} = \left. \frac{\partial(V_{fluid}/V_{total})}{\partial p} \right|_{boundary\ conditions} \quad (5.2)$$

Note that several specific storage coefficients can be defined: at constant volume S_ϵ , at constant stress S_σ or for uniaxial loading S_v . Because its easier to store fluid when the matrix has more freedom to deform, we get $S_\epsilon \leq S_v \leq S_\sigma$. Their unit is 1/Pa.

Hydrologists use other sets of storage coefficients:

1. The specific storage normalized relative to hydraulic head: $S_s = S_{boundary\ conditions} \times \rho_f g$, where ρ_f is the density of the fluid. Its unit is in 1/m.
2. The storativity S which is the specific storage in 1/m integrated over the thickness b of the reservoir:

$$S = \int_{z=0}^b S_s dz = \bar{S}_s b \quad (5.3)$$

- Poroelastic expansion coefficients. They quantify how an expansion in volume of the whole medium results in a expansion in the volume of the pore. One of them is the Biot-Willis coefficient:

$$\alpha = \left. \frac{\partial(V_{fluid}/V_{total})}{\partial \epsilon} \right|_{pressure} = 1 - \frac{K}{K'_s} \quad (5.4)$$

where K is the bulk modulus of the porous medium compared to the bulk modulus K'_s of the matrix².

- The difference between the drained and the undrained moduli is also related to the interaction between fluid and rock. For the drained case, the fluid pressure does not change. The response of the porous medium is controlled by the skeleton structure and its compliance. For the drained moduli, the fluid does not have time to escape from the pores and the small compressibility of the fluid enhances the rigidity of the porous medium. For instance, the undrained bulk modulus is related to the drained bulk modulus through $K_u = \frac{K}{1-\alpha B}$.

The Skempton coefficient and the specific storage are the ones widely used in interpreting tidal parameters. The specific storage is used in the hydraulic diffusivity and in the tidal efficiency of equation (5.7).

As the pure elastic medium may be characterized by different sets of two parameters, a poroelastic medium is characterized by a set of four independent parameters, for instance K , ν , K_u and ν_u . Detournay and Cheng [1993] used the shear modulus G , α , ν and ν_u . The set α , B , K_u and ν_u is easily obtainable with tidal analysis.

Beyond these macroscopic parameters, there is a micromechanical description of the porous medium. The relation between fluid and the matrix is due to the presence of the pores. Two major factor influence the effect of the pores on the elastic modulus: their importance (expressed by the porosity ϕ) and their compliance. The compressibility $1/K_f$ of the fluid is a third parameter which

²The strict definition of K'_s is that it is the change in volume of the matrix when the fluid pressure is equal to the confining pressure. The matrix skeleton is loaded from the exterior boundaries of the samples but also from its internal pores. In practice, this configuration happens when the sample isunjacketed and confining fluid can enter the sample. Hence, K'_s is also labeled the unjacketed bulk modulus). Note that even if the material constituting the matrix is incompressible, it is still possible to deform the pores by keeping the volume of matrix constant.

| α | B | K_u | S_σ | S_v | S_ϵ |
|----------|----------------------------|-----------------------------|----------------------------------|------------------------------------|--------------------|
| 1 | $\frac{K_f}{\phi K + K_f}$ | $\frac{\phi K + K_f}{\phi}$ | $\frac{1}{K} + \frac{\phi}{K_f}$ | $\frac{1}{K_v} + \frac{\phi}{K_f}$ | $\frac{\phi}{K_f}$ |

Table 5.1: Simplified expression of the poroelastic coefficients in the case of an incompressible matrix (from [Wang, 2000, Tab. 3.2])

influence the stiffness of the porous medium. The fluid is assumed not change the shear rigidity of the porous medium.

If the stiffness of the matrix is very large, the set of parameters describing the porous medium may be reduced to the three parameters K , ϕ and K_f and the rigidity of the medium. For this case, we get table 5.1, that is derived from [Wang, 2000, Tab. 3.2].

We will see that the tidal response provides essential information about the new parameters relative to the pore that were added in addition to a pure elastic case.

Poroelastic information provided by the tidal analysis

General case In a *confined* reservoir³, the volumic strain ϵ in the formation is converted into a pressure change p in the formation through the formula

$$p = B K_u \epsilon \quad (5.5)$$

$B K_u$ is called the *tidal efficiency*. If the fluid level in the borehole directly records the pore pressure in the medium, we get directly the product $B K_u$.

It is relatively easy to verify this assumption: the phase lag should be null (once the oceanic loading has been subtracted). The assumption is more probable to be met for a closed well than for an open well, because less fluid is required for the well to match the variations of the pore pressure in the formation (see section 5.2).

Moreover, if you have the barometric data, you can get the barometric efficiency γ :

$$p = \gamma p_{atm} = \frac{B(1 + \nu_u)}{3(1 - \nu_u)} p_{atm} = \frac{\alpha}{K_v S_v} \quad (5.6)$$

where $K_v = 3K \frac{1-\nu}{1+\nu}$ is the uniaxial modulus. The parameter γ is called the *barometric efficiency*.

You can then get two coefficients out of the four necessary to fully describe the porous medium. Other data, as sonic, log could provide the supplementary parameters like the undrained moduli K_u and ν_u . In the case of the AIG10 borehole of the Corinth Rift Laboratory, a good knowledge of the oceanic tides enabled us to get the oceanic loading and to determine all the poroelastic parameters. The major advantage of this method is that the poroelastic parameters are estimated at a large scale. This scale is more relevant for reservoir production, than the local properties obtained by borehole logging.

Rigid matrix approximation If you make the assumption of a rigid matrix, equations. (5.5) and (5.6) reduce to [Wang, 2000, Tab. 3.2]:

$$p = \frac{K_f}{\phi} \epsilon \quad (5.7)$$

$$p = \frac{K_f}{K_f + \phi K_v} p_{atm} \quad (5.8)$$

³The not purely confined case is addressed in section 5.2 on the hydraulic response.

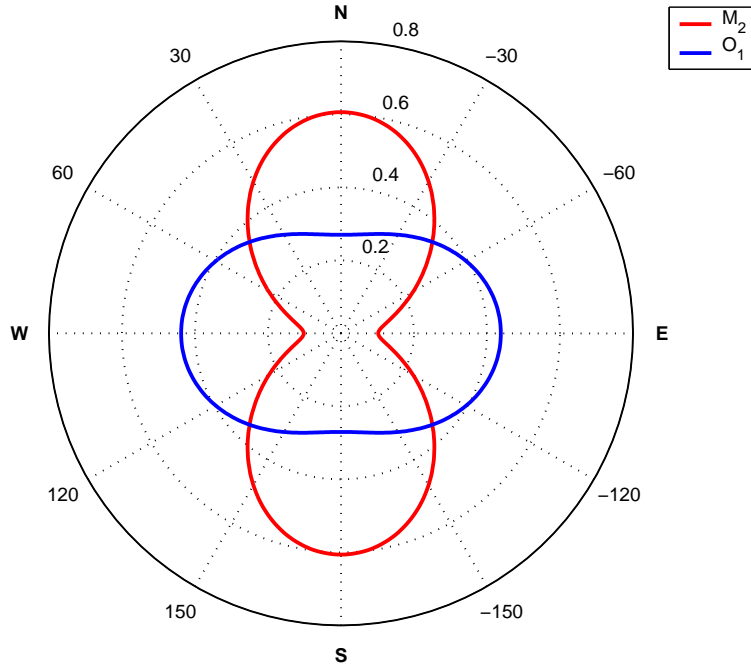


Figure 5.2: Distribution of the deformations as a function of the azimuth for the O_1 and M_2 constituent. Figure redrawn from Melchior [1983], with only an expansion of equation (2.4) to the order 2.

If you already know K_f , you get directly ϕ from the tidal response. With the barometric response, you get also K_v .

If moreover, you assume that the matrix and the pores are not deformable, $S_\sigma = S_v = S_\epsilon = S_s = \phi/K_f$. We then get

$$p = \frac{\epsilon}{S_s} \quad (5.9)$$

$$p = p_{atm} \quad (5.10)$$

5.1.2 Fractured medium

If the response of the well is controlled by a single fracture, the pore pressure is only sensitive to the tidal stress/strain normal to the fracture. It becomes a directional strainmeter [Bower, 1983].

As the strain amplitude are different between the diurnal and semi-diurnal wave (figure 5.2), the comparison of the amplitude of the tidal parameters at these frequencies should give more information on the orientation of the fracture.

There are three parameters in these problems: the dip and azimuth of the fracture, and its compliance. Theoretically, you can solve fully the problem by using also the response to the barometric loading, in addition to the amplitude of the M_2 and O_1 constituents⁴.

⁴As the response is assumed to be fully elastic, there should be no phase lag (after removal of the oceanic loading effect.)

5.2 Hydraulic response and permeability

We need also a parameter describing the ease with which the fluid circulates within the medium. One evident choice is the permeability k , defined as the empirical factor relating the fluid flow q in m^3/s to the gradient in pressure p :

$$q = -\frac{k}{\eta} \vec{\nabla} p \quad (5.11)$$

The permeability only reflects the properties of the matrix. In this formulation, the fluid properties appear explicitly through the dynamic viscosity η .

Some other expressions are often encountered in the hydrological literature:

1. The hydraulic conductivity C , which is the permeability normalized by the properties of the transported fluid. Its derived from the permeability k through the equation $C = \frac{k \rho_f g}{\eta}$, where ρ_f is the density of the fluid, η , the dynamic viscosity of the fluid and g , the gravity acceleration. The units of the hydraulic conductivity C is in m/s . Its is convenient to use when dealing with hydraulic head instead of pressure.
2. The transmissivity T which is the hydraulic conductivity C integrated over the thickness b of the reservoir: $T = \bar{C}b$.

$$T = \int_{z=0}^b C dz = \bar{C}b = \frac{\bar{k}, \rho_f g}{\eta} b \quad (5.12)$$

The transmissivity units are m^2/s .

The permeability of the reservoir may affect the tidal response, primarily through the phase. Conversely, the study of the tides provides information on the permeability of the system, if the poroelastic response has been already evaluated by independent means.

5.2.1 Fluid flow to the well

The well monitors pressure changes related to tidal strain because the porous medium supplies fluid to it. If the permeability of the medium is too small, then the well responds with delay. The amplitude of the fluid level oscillations also drops as the reservoir cannot supply enough fluid for the well to match the pressure.

This qualitative description has been quantified by Hsieh et al. [1987]. We present here a simplified (but still rigorous) version of his equations. Like Hsieh et al. [1987], we will express our results with hydraulic head h as a proxy for pressure, as it is a quantity equivalent to the fluid level measured in the well.

Let us consider the geometry of figure 5.3. The tidal strain is modeled as a dilatational strain $\epsilon(t)$ applied uniformly on an homogeneous isotropic reservoir. It induces a change in hydraulic head related to the poroelastic properties of the formation. Because of its rigid casing, a well not open to the formation is not intrinsically disturbed by the tidal waves. But, if the well is open or screened, the fluid level in the well h_w has to fit the hydraulic head h in the formation. In practice, the change in pressure is possible thanks to a fluid volume provided by the formation : if the formation were impermeable, the well would not experience any fluid level change, like a fully cased well. If the formation is poorly permeable, the fluid level in the well is out of equilibrium and would not match the far field hydraulic head in the formation. Hence, a fluid flow occurs in the formation near the well.

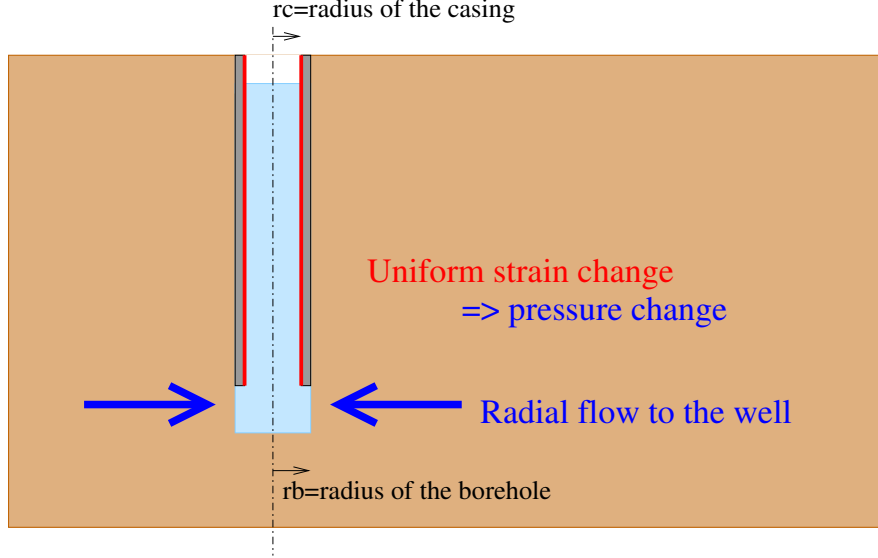


Figure 5.3: Flow to the well in a porous medium, with the hypothesis underlying the model of Hsieh et al. [1987].

Quantitatively, the evolution of hydraulic head is controlled by the set of equations

$$\frac{\partial^2 h}{\partial r^2} + \frac{1}{r} \frac{\partial h}{\partial r} + \frac{B K_u S}{\rho g T} \frac{\partial \epsilon}{\partial t} = \frac{S}{T} \frac{\partial h}{\partial t} \quad (5.13)$$

$$\rho g h(r \rightarrow \infty) = B K_u \epsilon \quad (5.14)$$

$$h(r = r_b) = h_w \quad (5.15)$$

$$2 \pi r_b T \left. \frac{\partial h}{\partial r} \right|_{r=r_b} = \pi r_c^2 \frac{\partial h_w}{\partial t} \quad (5.16)$$

where B is the Skempton coefficient (equation (5.1)), S the storativity of the reservoir (equation (5.3)), T the transmissivity of the reservoir (equation (5.12)), r_c the radius of the casing in which the fluid level rises and r_b the radius of the well where the fluid flow enters the well. Equation (5.13) describes the fluid diffusion, with the tidal loading as a source term. Equations (5.15) and (5.16) describe the continuity of the hydraulic head at the well radius and the conservation of mass. Equation 5.13 is simplified when we define the quantity $s = h - \frac{B K_u \epsilon}{\rho g}$, and consider a forcing oscillation in the form $\epsilon = \epsilon_0 e^{i\omega t}$. Because the equations 5.13 to 5.16 are linear, the solution is of the form $s = s(r, \omega) e^{i\omega t}$

$$\frac{\partial^2 s(r, \omega)}{\partial r^2} + \frac{1}{r} \frac{\partial s(r, \omega)}{\partial r} = \frac{i S \omega}{T} s \quad (5.17)$$

$$s(r \rightarrow \infty, \omega) = 0 \quad (5.18)$$

$$s(r = r_b, \omega) = h_w(\omega) - \frac{B K_u \epsilon_0}{\rho g} \quad (5.19)$$

$$2 \pi r_b T \left. \frac{\partial s(r, \omega)}{\partial r} \right|_{r=r_b} = i \omega \pi r_c^2 h_w(\omega) \quad (5.20)$$

The solution to equation 5.17 is $s = C_I I_0(r\sqrt{i\omega S/T}) + C_K K_0(r\sqrt{i\omega S/T})$. Equation (5.18) requires that $C_I = 0$. We have then two unknowns to solve, C_K and $h_w(\omega)$ with the two equations

5.19 and 5.20. We then get:

$$h_w(\omega) = \frac{\frac{B K_u \epsilon_0}{\rho g}}{1 + \frac{r_c^2}{r_b^2} \frac{r_b \sqrt{i\omega S/T}}{2S} \frac{K_0(r_b \sqrt{i\omega S/T})}{K_1(r_b \sqrt{i\omega S/T})}} \quad (5.21)$$

There are three regimes as shown in figure 5.4.

1. When the transmissivity is large or the frequency of the pressure change in the formation is small, the fluid level perfectly matches the pore pressure: the relative amplitude is equal to one, with no phase lag. The well is hydraulically coupled to the formation and is well described by equation (5.5) $B K_u$ can be recovered from the amplitude response.
2. If the transmissivity T lies between r_b^2/τ and $1000 r_b^2/\tau$ (τ is the period of the tidal oscillation), then the phase lag of the well level oscillation increases rapidly. The amplitude decays more slowly. Permeability can be recovered from phase lag (see below).
3. If the transmissivity of the formation is very small, the amplitude of the oscillation is very small. A smaller amount of fluid is necessary to fill the well (equation (5.20)), and the phase lag saturates. The amplitude continues to decay with smaller transmissivity. Thus, at very low permeability, a very good precision sensor is needed to perceive at least 1/4 of the amplitude of the oscillation in the well. As a reminder, for a non hydraulically damped well, the minimal resolution is of 200 Pa. If you work in this regime, it is still possible to derive hydraulic information on the reservoir from the amplitude response but you need an excellent pressure sensor. The signal over noise ratio is also smaller.

When the well is in regime 2, the transition regime, the assessment of the phase lag of the well provides an excellent tool to estimate the hydraulic properties. For a water aquifer, this regime is attained for a permeability comprised between $10^{-16} \text{ m}^2 = 0.1 \text{ mD}$ and $10^{-13} \text{ m}^2 = 0.1 \text{ D}$. For an oil reservoir⁵ tapped over 100 m by a well of radius 10 cm, this regime is attained for permeability comprised between $10^{-15} \text{ m}^2 = 1 \text{ mD}$ and $10^{-12} \text{ m}^2 = 1 \text{ D}$.

Equation (5.21) holds for the barometric pressure by replacing $\frac{B K_u \epsilon_0}{\rho g}$ by γp_{atm} in a closed well or by $(1 - \gamma)p_{atm}$ for a vented sensor in an open well. For a non-vented sensor in an open well, you cannot get directly the shape of the Hsieh equation, since you measure $p = \rho_f g h_w + p_{atm}$. You have to subtract first the atmospheric pressure to estimate the spectral response of the well to a volumic strain through the barometric response.

If you operate in a closed well, the wellbore storage is reduced. In equation (5.20), the term πr_c^2 is replaced by $\frac{V}{K_f} \rho_f g = \pi r_c^2 \frac{L}{K_f} \rho_f g$, where L is the length of the screened region. For $L = 100 \text{ m}$, the wellbore storage is decreased by 1000. For $L = 1 \text{ m}$, the wellbore storage is decreased by 10^5 . The criteria in transmissivity for the coupled, transitional and uncoupled regime is shifted by dividing the limit transmissivity by the increase in specific storage. It is easier to be in a coupled regime, where there is not head gradient around the well. The response of the well is described by equation (5.5) and the parameter $B K_u$ can be recovered, but not the permeability.

5.2.2 Diffusion at the boundaries of the reservoir

In section 5.1.1, we only discussed the case of a confined reservoir. What happens if the reservoir is not confined?

⁵We assume that the crude oil has a kinematic viscosity $\eta/\rho = 10^{-5} \text{ m}^2/\text{s}$, typical of a Norway crude oil at 20°C.

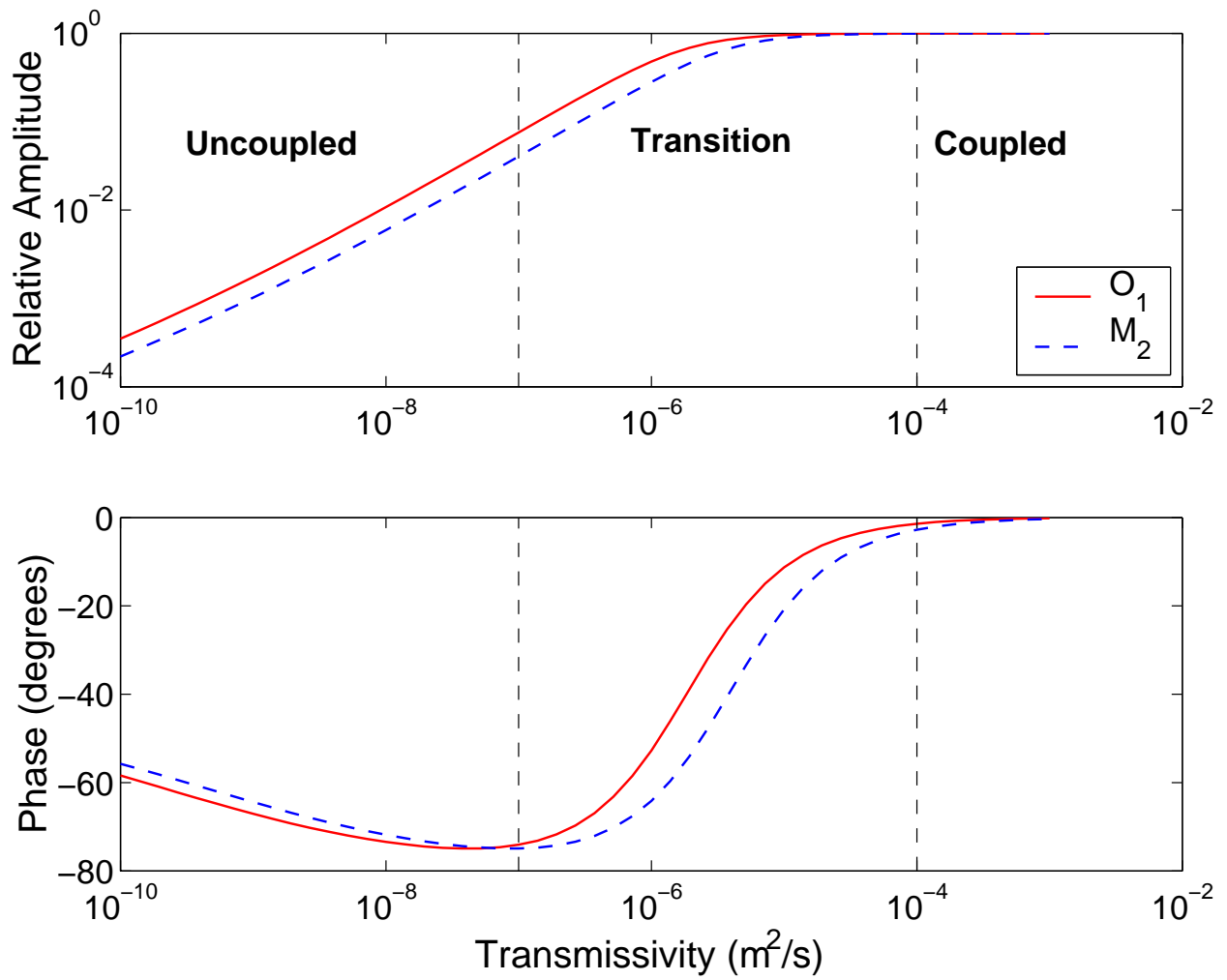


Figure 5.4: Predicted amplitude and phase (lags negative) of the response of a reservoir to tides. We used here a storativity of 10^{-4} and a well where $r_b = r_c = 10$ cm.

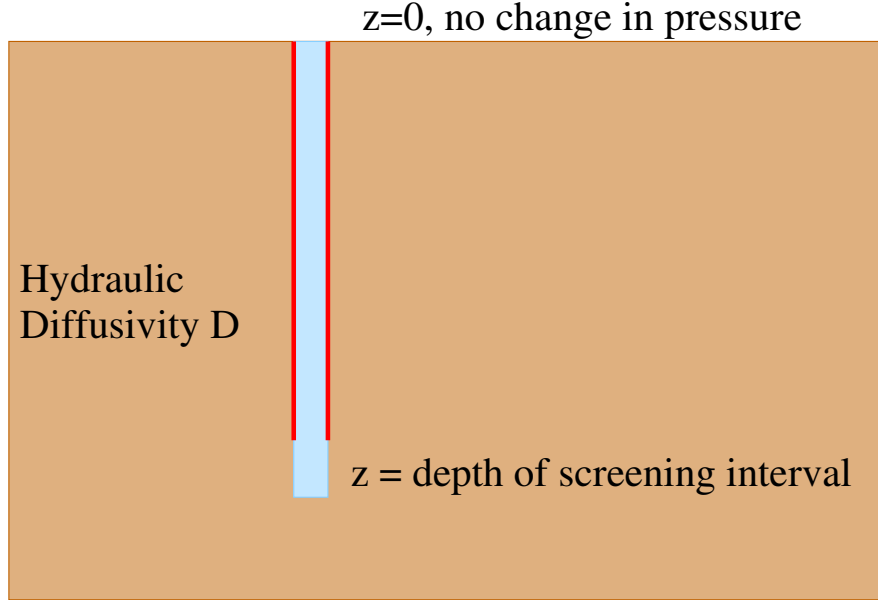


Figure 5.5: A case of diffusion of the pressure to the surface. Here, the reservoir is poorly permeable and confines itself (right).

The strongest effect is the connection with the water table [Roeloffs, 1996]. The surface of the Earth is a free surface and there is no change in fluid level. The tidal amplitude dies out as the pressure diffuses to the surface. At small frequencies, the skin length may exceed the depth of the screened interval in which the well pressure is measured.

Lets consider the case of figure 5.5. We will assume that the flow in the confining formation is purely vertical:

$$D \frac{\partial^2 p}{\partial z^2} + B K_u \frac{\partial \epsilon}{\partial t} = \frac{\partial p}{\partial t} \quad (5.22)$$

$$p(z \rightarrow \infty) = B K_u \epsilon \quad (5.23)$$

$$p(z = 0) = 0 \quad (5.24)$$

$$(5.25)$$

Equation (5.22) is the diffusion equation for pressure with a source term due to the tidal forcing. Equations (5.23) and (5.24) gives the boundary conditions at the surface and at great depths, where the diffusion to the surface is negligible.

The general solution of equation (5.22) is $p = B K_u \epsilon + C_1 e^{(1+i)z/\delta} + C_2 e^{-(1+i)z/\delta}$, where $\delta = \sqrt{\frac{2D}{\omega}}$. With the two limit equations (5.23) and (5.24), we get the solution

$$p(z, \omega) = B K_u \epsilon \left(1 - e^{-(1+i)z/\delta} \right) \quad (5.26)$$

The resulting spectral response is visible in figure 5.6. In contrast to the wellbore storage effect, the phase are positive. Also, here only the hydraulic diffusivity is important.

The expression of the barometric pressure is different for a non-vented sensor in an open well:

$$p(z, \omega) = p_{atm} \left(\gamma - (1 - \gamma) e^{-(1+i)z/\delta} \right) \quad (5.27)$$

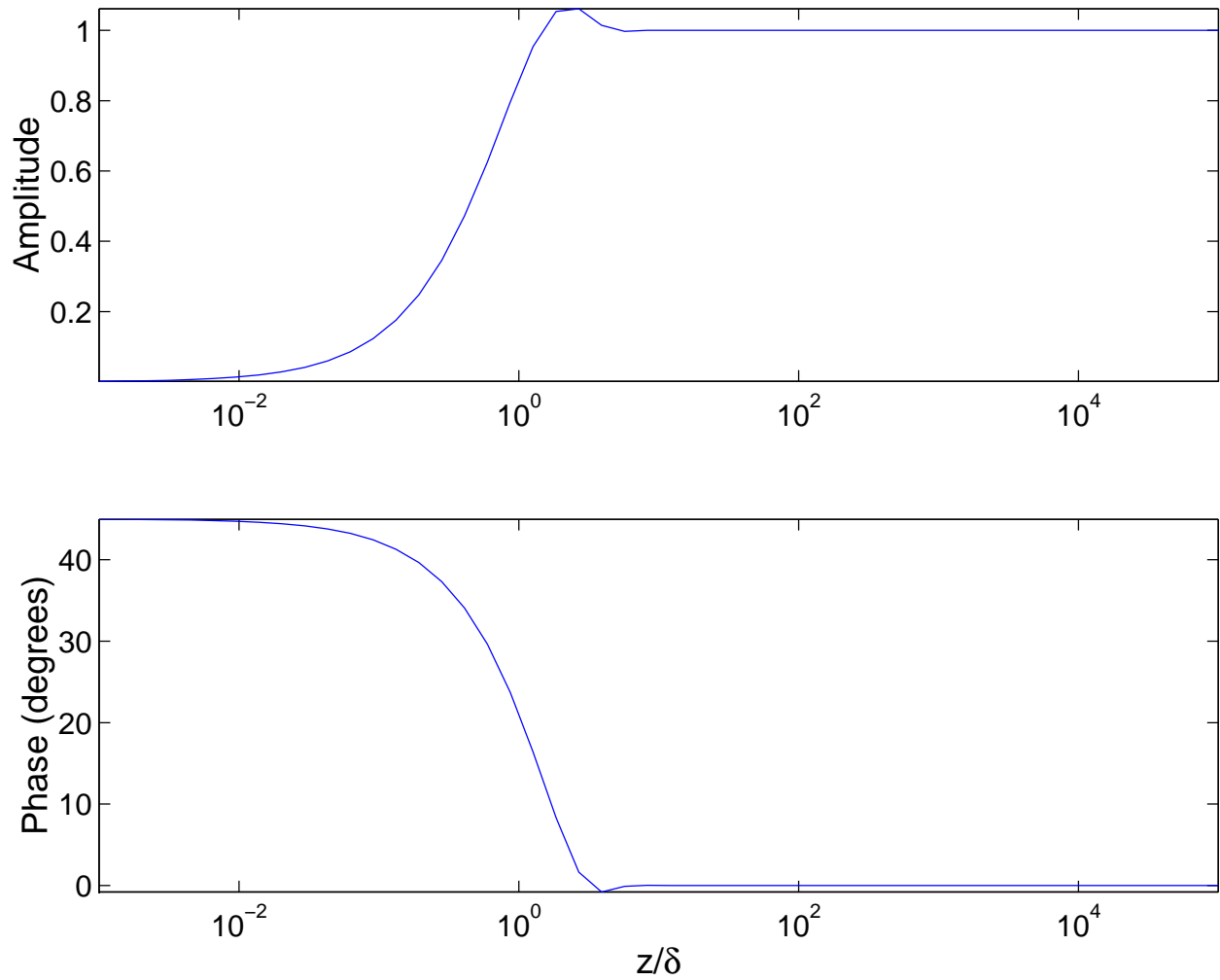


Figure 5.6: Amplitude and phase (lags negative) of due to the diffusion of the pressure to the surface as described in figure 5.5.

but not for a vented sensor in an open well

$$h(z, \omega) = \frac{p(z, \omega) - p_{atm}}{\rho_f g} = -(1 - \gamma) \frac{p_{atm}}{\rho_f g} \left(1 - e^{-(1+i)z/\delta}\right) \quad (5.28)$$

5.2.3 Non uniform loading

If there is surface loading that is heterogeneous, the induced pressure field is not uniform. The gradient in pressure induces a fluid flow, which modifies the response of the reservoir. If you know well the loading and the boundary condition, the hydraulic properties can also be retrieved from tidal analysis. This technique has been applied for the AIG10 borehole of the Corinth Rift Laboratory, where the loading of the Gulf of Corinth has been computed at depth with the Boussinesq equation [Doan, 2005]. This enabled us to get the permeability of a karstic reservoir, which could not have been obtained by a direct hydraulic test on the well. The permeability was so high that the fluid flow out of the borehole was limited by the head loss in the borehole.

Chapter 6

Example: Change in hydraulic properties with time at the Piñon Flat Observatory

6.1 Data presentation

Strain monitoring has been performed in the The Piñon Flat Observatory for more than 20 years. Part of the project consists in water level monitoring.

We will show that the response of the well is controlled by the hydraulic properties of the well, so that the tidal analysis directly provides hydraulic properties through time. These wells were studied by Elkhoury et al. [2006]. The objective of the analysis is to check the persistence of the tidal response of the well through time. We will therefore make the analysis on short time spans at the expense of the resolution of the tidal parameters. In other words, we will have a good time resolution, at the expense of a full poroelastic characterization.

6.1.1 Data

We have the minimal data necessary for the analysis:

- More than 20 years of water level data.
- The exact location and the time of these data (in UT).

We use also the barometric pressure. The data from the site have already been presented during the discussion of barometric pressure in figure 3.1 and 3.2. The negative correlation between water level and barometric pressure confirms that the data are pure water level data.

The site is located more than 100 km from the seashore. We do not need a tide gauge to estimate accurately the oceanic loading. We will use some SPOTL to estimate the correction to the tidal response while inverting the tidal response into quantitative values of the properties of the medium tapped by the well.

6.1.2 Barometric response

Figure 6.1 shows the transfer function estimate. Within the frequency band of the tides, the amplitude decays with frequency whereas the phase lag increases with frequency. This is the behavior

expected when the well response is dominated by the fluid flow to the well. For comparison, the best fit with the Hsieh model (equation (5.21)) is shown with thick yellow lines: the trend is similar. The discrepancy between the model and the data is to be due to the fractured medium surrounding the PFO wells, different from the porous medium underlying the Hsieh model of equation (5.21).

The above spectrum shows that the pressure cannot be removed accurately by a simple subtraction of the barometric pressure data [Quilty and Roeloffs, 1991]. The response method implemented by BAYTAP enables the user to take into account better this complex response [Matsumoto et al., 2003]. Other software make only frequency-independent correction of pressure, and it is advised to the pressure before performing the analysis. But you risk applying a wrong coefficient.

6.1.3 Preparation of the data

We resample the 5-minute data at hourly intervals. The accuracy of the time domain analysis is not very sensitive to the sampling interval, as long it is less than hour and resampling reduces the duration of the computation. Incidentally, it also avoids cumulative errors in time labeling of the data (5 minutes=1/12 hour, and 1/12 is not a decimal number.).

The data are not despiked. We will show the first attempt to characterize the change in tidal response. If we see an outlier, it may either be due to locally spiky data or to a short-duration change in tidal response, and we will have to refine the analysis with a better preprocessing of the data. Here we target only persistent changes in tidal response.

6.2 Analysis

The analysis is performed with BAYTAP. Typical input file is shown in the example file of appendix D. We use the functionality of BAYTAP to split the data into 30 days times spans. The tidal waves are grouped in 5 constituents, O_1 , K_1 , M_2 , S_2 , M_3 . To illustrate the need for a full response function to barometric pressure, we will conduct two analyzes: one with LAGP=0 (shown with blue points in figure 6.2), another with LAGP=12 (shown with red points in figure 6.2).

Figure 6.2 shows the obtained tidal response for all the inverted constituents. The computation time is about 2 minutes on a 2.6 GHz Linux machine.

Let us first check the correctness of the analysis, by making some rapid assessment of the order of magnitude of the quantities obtained:

- The gain is of about 5 GPa (to get this value, we used equation (2.17) with $h = 0.606$, $l = 0.0840$ and $\nu = 0$). If the water level directly matched the pore pressure in the formation, we would get directly the quantity $B K_u$, where B is the Skempton coefficient (between 0.3 and 0.8), and K_u is the undrained bulk modulus. The quantity we obtained is of the correct order of magnitude, although a little small. This small amplitude is normal since the amplitude response is dampened by the poor permeability of the formation drilled.

Curiously, the O_1 tide has a smaller response amplitude than that of M_2 tide. This seems to be in contradiction with the barometric response of figure 6.1. In fact, the response of the well is dominated by a set of horizontal fracture. The apparent discrepancy between the amplitude of O_1 and M_2 is due to the anisotropy of the medium.

- The phase is shifted by 180° . This is due to the sign convention used for strain by the program. When the reference theoretical strain are computed, an increase in strain accounts for a dilatation, which should results in a decrease in pore pressure, giving a prefactor $-1 = e^{i\pi}$.

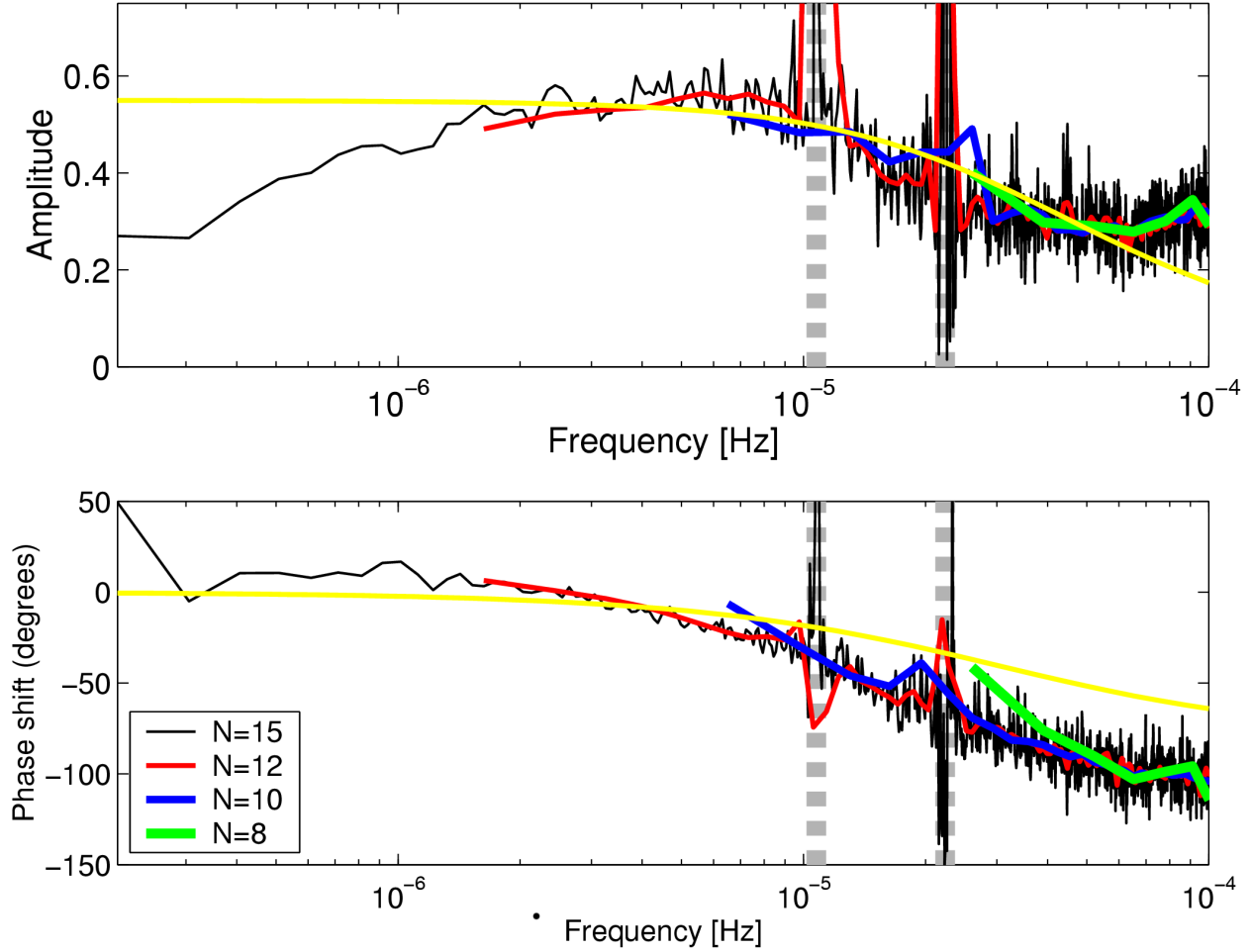


Figure 6.1: Transfer function estimate of the response of well CIB of the Piñon Flat Observatory to *relative* pressure from 1987 to 1992. To reduce noise error, the output y (here the water level) and the input x (here the barometric pressure) are split in spans of 2^N samples. The spectral density P_{xx} and the cross spectral density P_{xy} are averaged over the spans [Lyons, 2004]. The transfer function is estimated as the P_{xy}/P_{xx} [Buttkus, 2000]. Smaller N give less noisy transfer function estimate because the average involve more spans of data, but lower frequencies are not estimated. Therefore, a variety of values of N are considered. For comparison, the best fit of Hsieh model are displayed in continuous yellow lines. The frequency corresponding to the O_1 ($f \sim 1.0 \times 10^{-5}$ Hz) and to the M_2 ($f \sim 2.2 \times 10^{-5}$ Hz) tides are drawn as vertical dashed gray lines.

Otherwise, the phase lies below 180° , denoting a delay, as expected from the Hsieh equation (5.21) and from figure 4.2.

Which component should you trust?

S_1 and S_2 are solar tides. They are polluted by several side effects: changes in pressure as well as in temperature. K_1 (very close to S_1 , see figure 3.2) is then problematic to analyze.

M_3 has a very small amplitude compared to the diurnal and semi-diurnal constituent (see figure 4.2). Its interpretation is therefore to be taken with caution. Notably, the phase is expected to be very noisy.

The favorite constituents to analyze are therefore O_1 and M_2 . From these two waves, M_2 is better characterized, as more oscillations are in this time span. The characterization of O_1 is more dependent of a correct removal of the barometric pressure. Compare the stability of red curve where pressure has been removed with a memory enabled $LAGP > 0$ to the case where pressure is assumed to apply instantaneously $LAGP = 0$.

6.3 Discussion

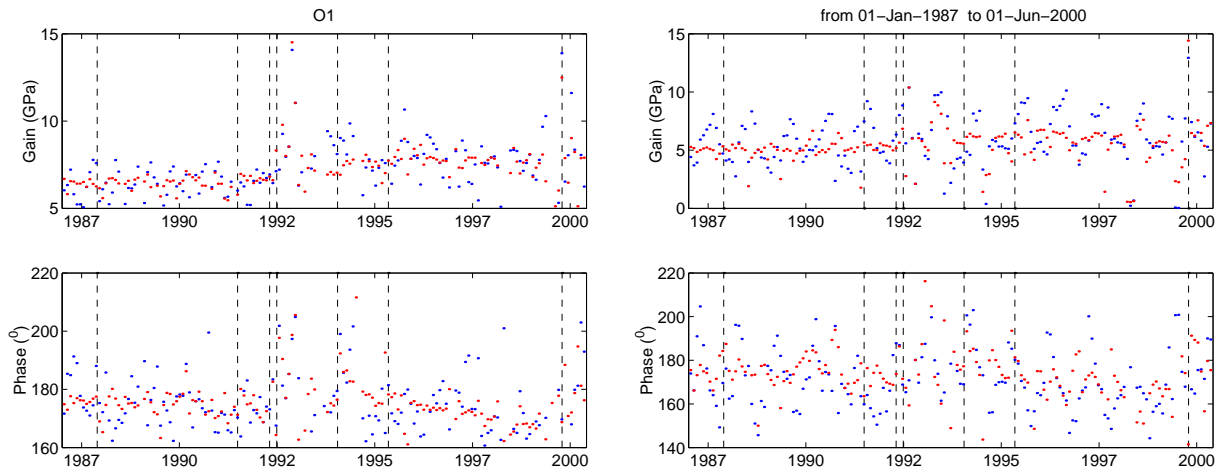
The M_2 component in figure 6.2 shows striking changes in both amplitude and phase. What happens? Is it a change in the poroelastic properties? If so, only the amplitude would vary. Is it a change in the hydraulic properties? This hypothesis explains both the decrease in amplitude and in phase delay. The Hsieh equation (5.21) is dependent on only two parameters: the hydraulic transmissivity and storativity as done by Elkhoury et al. [2006].

The oceanic loading change induces a phase advance of 6° relative to the theoretical tides. The diffusion to the surface adds another phase advance of 7° . Once, these two effects are corrected, equation (5.21) gives an estimate of the permeability and storativity through time. The results are displayed in figure 6.3. The permeability is increased up to a factor four for the 1992 Landers earthquake. Meanwhile, the specific storage evolves much more smoothly. This confirms that the change in response of the well has hydraulic causes.

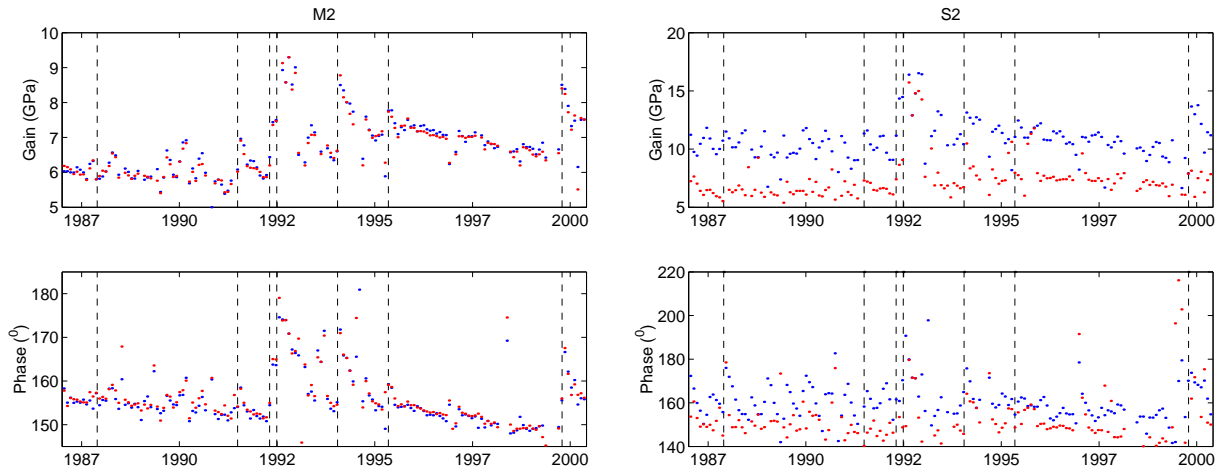
The O_1 tide also experiences some changes in phase, but not much in amplitude. Figure. 6.1 explains why. The diurnal frequency is at the onset of the decline in amplitude while the phase lag is already important. Altering slightly the permeability will produce subtle changes in amplitude, but a clear reduction in phase lag. A more detailed analysis and its implication is detailed in Elkhoury et al. [2006].

Although we performed here a crude analysis by not despiking the data, we could demonstrate long-term disturbance in tidal response, related to permeability enhancement by seismic waves.

Diurnal waves



Semi-Diurnal waves



Ter-Diurnal waves (M3)

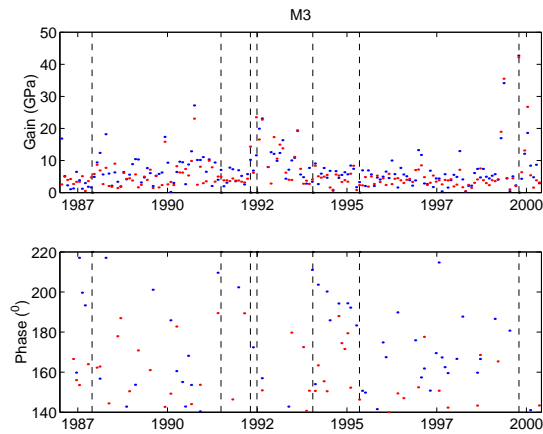


Figure 6.2: Tidal response of the water level in the CIB of Piñon Flat Observatory. We used spans of hourly data lasting 30 days and conducted an inversion for 5 constituents (O_1 , K_1 , M_2 , S_2 , M_3). Major earthquakes are denoted with dashed lines.

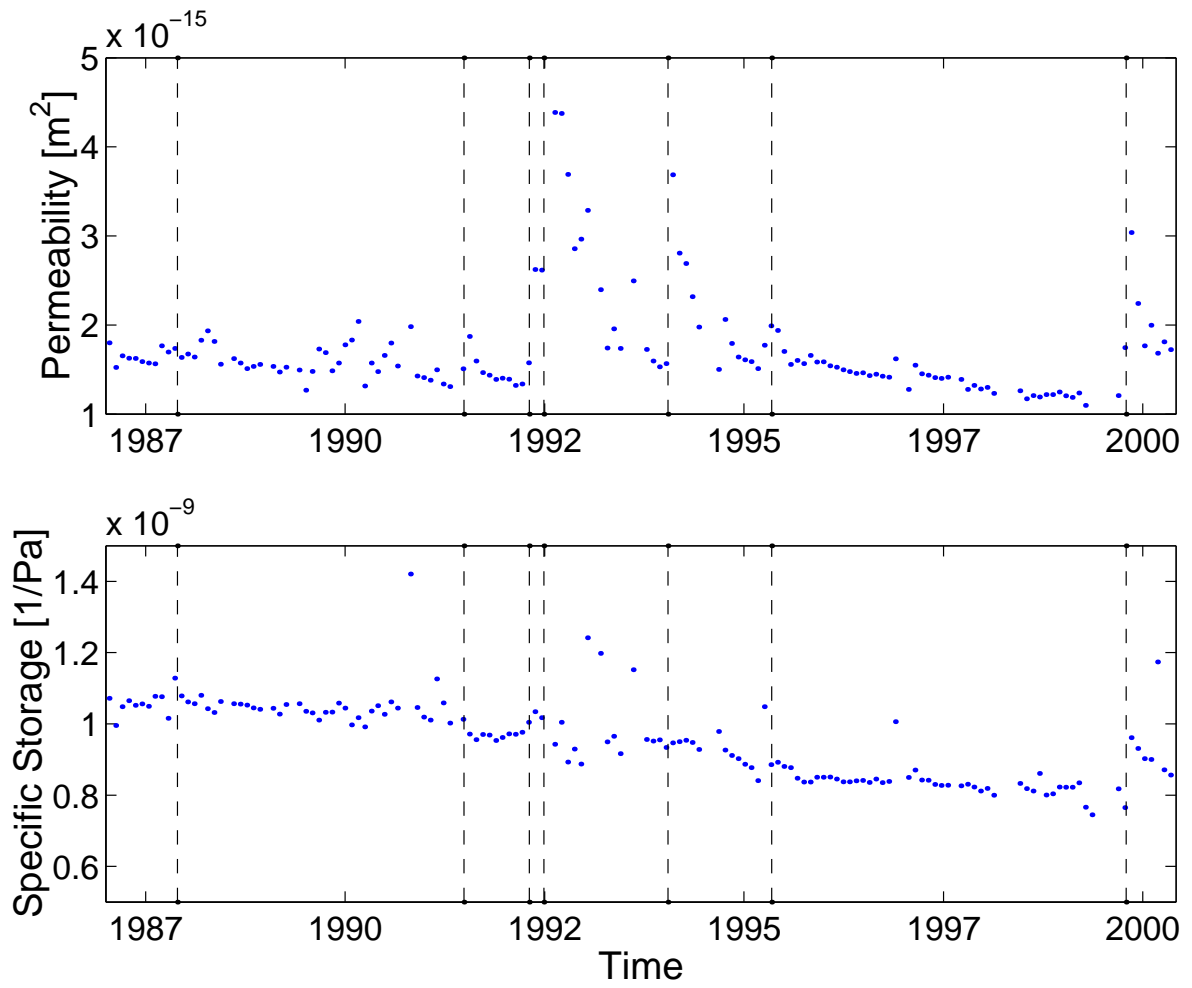


Figure 6.3: Permeability and specific storativity computed from equation (5.21) with the tidal response of the M_2 tides.

Chapter 7

Conclusion

Earth tides induce measurable changes in pressure in boreholes. As tides can be predicted with great accuracy, the response of the borehole to the tidal forcing can be retrieved quantitatively. If the formation tapped by the borehole is permeable enough, the tidal response provides For smaller permeabilities, the amplitude and phase of the tidal response give both the poroelastic parameters and the permeability of the reservoir.

Tidal analysis is a cheap, non-intrusive tool to measure the reservoir tapped by the well at large-scale. The effective permeability can be recovered as a function of time, as well as the poroelastic parameters in the appropriate regime.

Appendix A

Glossary

Areal strain Deformation within a horizontal plan. It is the sum of two horizontal strains computed for two orthogonal horizontal directions.

Barometric pressure Pressure at the base of the atmosphere.

Doodson numbers Tidal waves classification, with numbers labeling a tidal waves, indicating the influence of (1) the Earth rotation, (2) of the revolution of the Moon around the Earth, (3) of the revolution of the Earth around the Sun, of the changes in the Moon orbit via its (4) perigee and (5) its nodes and (6) finally by the change in the perihelion of the Earth.

Ecliptic plane Plane along which the planets of the solar systems are aligned. The Moon orbit is tilted by 23° to the ecliptic plane (see obliquity).

Ephemeris Tables or formula enabling the computation of the movement of the celestial bodies.

Free Core Nutation One of the resonance of the core rotation. Also named “Nearly Diurnal Free Wobble” or “Core Resonance”.

Gravity acceleration Earth exerts a force $\vec{F} = m\vec{g}$ on an object of mass m . \vec{g} is the gravity acceleration. It sums up 3 effects: the Earth gravity, the centrifugal force induced by the Earth rotation and the small gravity effect of other objects of the Solar system.

Hydraulic head Formation pressure removed from the hydrostatic pressure and expressed in a equivalent height of fluid: $h = (p - \rho_f g z) / (\rho_f g)$.

Hydraulic conductivity A permeability normalized by the properties of the transported fluid. The hydraulic conductivity is derived from the permeability k through the equation $C = \frac{k \rho_f g}{\eta}$, where ρ_f is the density of the fluid, and η is the dynamic viscosity of the fluid. g is the gravity acceleration. The units of the hydraulic conductivity C is in m/s. The hydraulic conductivity is convenient to use when dealing with hydraulic heads instead of pressure.

Hydraulic diffusivity Parameter controlling the diffusion of the pressure. The hydraulic diffusivity is equal to the ratio of the hydraulic conductivity over the specific storage of the medium. Its units are in m^2/s .

Moon node Intersection point of the Moon’s orbit and the ecliptic plane.

Obliquity Angle of the orbit of the Moon around the Earth and the ecliptic plane. About 5° , but it varies with time.

Perigee Point of an orbit around the Earth. This is the closest point from the Earth.

Perihelion Point of an orbit around the Sun. This is the closest point from the Sun.

Skempton coefficient Poroelastic parameter, describing the build-up of pressure Δp under an increasing of confining pressure $\Delta\sigma$ for an undrained poroelastic medium of constant volume.

Specific storage Ability of the formation to store fluid. The specific storage is defined at the relative volume of fluid stored by the system with its fluid pressure is increased by 1 Pa. Its units are in 1/Pa.

Storativity Specific storage (in units of 1/m) integrated over the thickness of the reservoir. The storativity has no dimension.

Tidal catalog A list of tidal constituents, with their frequency (or its Doodson number), their amplitude and phase. Because of the length of the list, it is no more a list but a catalog.

Tidal component The kind of data measured. It can be gravity acceleration, tilt, strain, etc. The well pressure data is considered as an indirect measurement of strain.

Tidal constituent Describe either a tidal wave in a narrow sense or a tidal packet in a broad sense.

Tidal efficiency Ratio of the change in pressure in the formation to the tidal strain which induces it. In a porous medium, it is equal to $B K_u$, where B is the Skempton coefficient and K_u is the undrained bulk modulus.

Tidal packet A group of tidal waves, for which the tidal parameters are the same.

Tidal parameter Complex number (amplitude and phase) describing the response of the system to a tidal constituent.

Tidal potential Potential from which is derived the tidal gravity force.

Tidal wave A term of the tidal expansion. It has a specific frequency.

Tides The heterogeneous part of the gravitational attraction exerted by a planet on a celestial body. This causes the deformation of the celestial body (and if they exist, of its oceans).

Transmissivity Hydraulic conductivity integrated over the thickness of the reservoir.

Appendix B

ERTID

| | |
|------------------|--|
| Function | Theoretical tides computation |
| Source code | Fortran source code provided |
| License | Same as SPOTL. None specified |
| Operating system | Should work on every operating system (tested under UNIX, Linux) |
| Catalog | Cartwright, Taylor, Edden 1971,1973 |
| Pros | Easy to use (interactive program) |
| Cons | We need 2 files to get the horizontal strain |

ERTID is a program written by Duncan Agnew, IGPP, UC San Diego. It is part of the SPOTL program (appendix C).

B.1 Input

The parameters are entered interactively. Here are the sequence of questions to be answered:

1. *Start time*- - - (*year,day,hour*) Self explanatory. The time is UT time
2. *End time*- - - (*year,day,hour*) Self explanatory. The time is UT time
3. *Time interval (hours)*- Beware that the error in this parameter will accumulate, so do not type 0.083 if you want a 5 minutes data. Use more digits.
4. *Type t for theoretical tides, m for Munk-Cartwright coefficients* Type “t”.
5. *North latitude*- in degrees
6. *East longitude*- in degrees
7. *Number of gravity (0 to 1), tilt (0-2), and strain (0-3) tides wanted* Press the number of gravity data you want to compute, then press return. Redo it for the two remaining values. In our case, it will be (0,0,2), as the strain are computed for two orthogonal directions.
8. *Strainmeter azimuth(s) - positive clockwise from north* To get the areal strain, you will need to add two strains computed for two orthogonal azimuths. For instance, 0 and 90.
9. *Enter output filenames (total of 2)*

Appendix C

SPOTL

| | |
|-------------------|---|
| Function | Oceanic load computation |
| Source code | Fortran source code provided (the install script designed for unixoid systems) |
| License | None specified |
| Ocean tides model | Schwiderski, CSR3, FES95.2, GOT00, TPX06.2 as well as local models for California (San Francisco Bay and Gulf of California (names in the program Sea of Cortez)), Canada (Bay of Fundy) and Hawaii |
| Pro | Extensive documentation, Flexible use |
| Cons | Personally none, maybe an old model of Earth. |

C.1 SPOTL: Some Programs for Ocean-Tide loading

SPOTL is a set of programs to compute the oceanic load [Agnew, 1996]:

- `nloadf` is the program computing the oceanic load [Agnew, 1997].
- `loadcomb` enables the *combination* of the oceanic *loads* computed from different contributions (typically a global model and a refined model of the nearby coastlines). It simply adds the contribution and gathers them under the same header.
- `harprp` converts the load file into a tidal parameter file.

Some add-ons are related to body Earth tides:

- `ertid` computes theoretical Earth tides. The program is detailed in appendix B
- `hartid` computes the expected tides by combining the theoretical Earth tides with the tidal parameters describing the response of the system to the Earth tides.

Other programs help to explore the reference files of table C.1 to C.3.

- `oclook` provides information from an ocean-tide file (See table C.1).
- `modcon` and `mapcon` are used during the installation process to convert compressed ASCII data into binary data. They are not used routinely by the user.
- `mapcheck` to examine the fine-scale land-sea database.

Programs are called by command line from a terminal.

SPOTL is delivered with an excellent documentation, detailing the options, describing the model and the computation procedure and presenting some examples. In this part, we only summarize this documentation.

C.2 Using NLOADF

C.2.1 Options

The manual of `nloadf` presents how to call the program

```
nloadf stname lat lon ht modelfile greenfile g | l [polyfile [+ | -] ]
```

stname Name of the station (for self-documentation)

lat, lon Latitude and Longitude of the station, in degrees

ht Elevation, in meters.

modelfile Model of oceanic tides to be used. The file is of the form `constituent.model`. See table C.1 for a list of possible choice.

greenfile Model of elastic response for a point load (Green function). The response is computed from a model of elastic properties of Earth with the method of Farrell [1972]. See table C.2 for a list of possible options.

[l/g] The reference along which the tides is computed: either relative to the longitude of the local observation point or relative to the **G**reenwich meridian.

polyfile [+/-] Optionally, it is possible to discard an area or to restrict the study to an area. The area is described by a polygon on the map. The points are listed in a polygon files. See table C.3 for the list of available options.

The last option is useful if the global model is very coarse for the local mass of water and if a better local description of the oceanic tides is available.

In the first example of the documentation of Agnew [1996], the oceanic load at the station PFO is computed with the following script

```
#!/bin/sh

# oceanic load -> *.ld file (Example derived from the documentation of D.C. Agnew)
#   global minus Cortez
../bin/nloadf PFO 33.61 -116.45 1280 m2.csr3tr green.gbavap.std l poly.cortez - > pfo_global.M2
#   Cortez only
../bin/nloadf PFO 33.61 -116.45 1280 m2.cortez green.gbavap.std l poly.cortez + > pfo_cortez.M2
#   Both of the above
cat pfo_global.M2.load pfo_cortez.M2.load | ../bin/loadcomb c > pfo.M2.load
```

| Global models | | | | | | |
|---------------|--------------------------------|-----------|-----------------|-------------|----------------------|----------------------|
| Suffix | Model | Cell Size | Latitude Limits | Long Period | Constituents | |
| | | | | | Diurnal | Semi-Diurnal |
| .schw | Schwiderski | 1° | -78° - +90° | M_f | O_1, P_1, K_1, Q_1 | N_2, M_2, S_2, K_2 |
| .csr3tr | CSR 3.0 | 0.5° | -78° - +90° | | O_1, P_1, K_1, Q_1 | N_2, M_2, S_2, K_2 |
| .fes952 | FES 95.2 | 0.5° | -86° - +90° | | O_1, P_1, K_1, Q_1 | N_2, M_2, S_2, K_2 |
| .got00 | GOT 00.2 | 0.5° | -90° - +90° | | O_1, P_1, K_1, Q_1 | N_2, M_2, S_2, K_2 |
| .tpxo62 | TPX 06.2 | 0.25° | -90° - +90° | M_f, M_m | O_1, P_1, K_1, Q_1 | N_2, M_2, S_2, K_2 |
| Local models | | | | | | |
| Suffix | Model | Cell Size | Latitude Limits | Long Period | Constituents | |
| | | | | | Diurnal | Semi-Diurnal |
| .bfund | Bay of Fundy | 0.1° | | | O_1, P_1, K_1, Q_1 | N_2, M_2, S_2, K_2 |
| .cortez | Gulf of California | 0.1° | | | O_1, P_1, K_1, Q_1 | N_2, M_2, S_2, K_2 |
| .gefu | Strait of Georgia/Juan de Fuca | 0.1° | | | O_1, P_1, K_1, Q_1 | N_2, M_2, S_2, K_2 |
| .osuhaw | Hawaiian Islands/Ridge | 0.033° | | | O_1, P_1, K_1, Q_1 | N_2, M_2, S_2, K_2 |
| .sfbay | San Francisco Bay | 0.01° | | | O_1, P_1, K_1, Q_1 | N_2, M_2, S_2, K_2 |
| .sl | St. Lawrence River/Gulf | 0.1° | | | O_1, P_1, K_1, Q_1 | N_2, M_2, S_2, K_2 |

Table C.1: List of tidal models of oceans supported by SPOTL.

| Green function file | Method | Elastic structure of the Earth |
|---------------------|-----------|---|
| green.gbavap.std | Farrell72 | Gutenberg-Bullen model (upper layer = averaged crust) |
| green.contap.std | Farrell72 | Gutenberg-Bullen model (upper layer = continental crust). |
| green.ocenap.std | Farrell72 | Gutenberg-Bullen model (upper layer = oceanic crust) |

Table C.2: Green functions for oceanic loading, computed with the equations of Farrell [1972]. The Green functions are dependent on the elastic structure of the Earth. Only radial models are available, which is problematic for the laterally heterogeneous crust. Hence several approximations of the crust are proposed.

The first line computes the oceanic load induced by all the oceans, except the Gulf of California in Mexico.

The second line computes the loading due to the tides of the Gulf of California alone.

The third line adds the two contributions.

C.2.2 Output

Load file

```

S PFO 33.6090 -116.4550 1280.
O M2 2 0 0 0 0 0 CSR model 3.0, with >50% land cells removed
G GUTENBERG BULLEN GREENS FUNCTIONS JOB02Q 10/19/71
G Rings from 0.03 to 1.00 with spacing 0.01 - detailed grid used
G Rings from 1.05 to 9.95 with spacing 0.10 - detailed grid used
G Rings from 10.25 to 89.75 with spacing 0.50 - ocean model grid used
G Rings from 90.50 to 179.50 with spacing 1.00 - ocean model grid used
P Polygon to include the Gulf of California

```

| Polygon file | Description |
|--------------|--|
| poly.bfund | Bay of Fundy |
| poly.cortez | Gulf of California |
| poly.gefu | Strait of Georgia/Juan de Fuca |
| poly.hawaii | Hawaiian Islands/Ridge |
| poly.sfbay | San Francisco Bay |
| poly.sl | St. Lawrence River/Gulf |
| poly.tplimit | Limits of TOPEX/POSEIDON derived oceanic models. |

Table C.3: Regions that can be circumscribed by predefined polygon files.

```

P all polygon areas excluded
C Version 3.2 of load program, run at Sat Nov 11 11:05:00 2006
C closest nonzero load was 0.88 degrees away, at 33.15 -117.35
C 1 zero loads found where ocean present, range 6.25- 6.25 deg
L 1 Phases are local, lags negative
X
g 1.3407 -85.1776
p 7.7003 100.8230
d 1.4016 -125.6176 4.1664 -35.8058 3.0469 -73.4878
t 23.9649 -99.7540 26.0249 -56.2445
s 2.8650 50.0946 2.0145 171.6295 4.8550 117.8368

```

There is a header documenting the options chosen and their characteristics. All lines from the header begin with an uppercase letter that categorizes the information:

- **Station:** with its name and its location (latitude/longitude/elevation)
- **Oceanic model:** constituent and model
- **Green function,** with the name of the Green function and the grid used.
- **Polygons** that have been used to describe the geometry of the oceans.
- **Comment** on the version on the way the computation has been done
- **Lags convention.** Whether they are determined locally or relative to the Greenwich meridian. The sign convention is reminded.
- **X** closes the header

Then come the amplitudes and phases in degrees (lags are negative) for the following components:

- **gravity:** Amplitude units are μgal , positive for decreasing g .
- **potential height,** relative to the surface of the Earth. Amplitude units are millimeters, positive for up.
- **displacement:** east, north, up. Amplitude units are millimeters, positive for (east/north/up).
- **tilt:** east, north. Amplitude is in nanoradians.
- **strain:** north-south, east-west, vertical. Amplitude units are nanostrain ($= 10^{-9}$). A positive amplitude denotes extension.

Tidal parameter file

The information from the load file presented above can be transformed in a parameter file thanks to the program `harprp`

```
1
-116.455
 2 0 0 0 0 0   1.4960   81.89
-1 0 0 0 0 0   0.0000   0.00
```

The first two lines of the output file indicate that the phases are local, and give the longitude of the station. The subsequent lines give the Cartwright-Tayler version of the Doodson code for the tidal constituent (see table 2.2), and its amplitude and phase. The final line gives an impossible Cartwright-Tayler code, to indicate the end of the file.

Using a tide generation program `hartid`, it is then possible to compute the time series of the tides induced by the ocean and to add them to the theoretical Earth tides to get the reference tidal strain.

C.3 Summary

Here is a script to compute the oceanic load time series corresponding to the M_2 constituent:

```
#!/bin/sh

# oceanic load -> *.load file (Example taken from the documentation of D.C. Agnew)
#   global minus Cortez
nloadf PFO 33.609 -116.455 1280 m2.csr3tr green.gbavap.std 1 poly.cortez - > pfo_global.load
#   Cortez only
nloadf PFO 33.609 -116.455 1280 m2.cortez green.gbavap.std 1 poly.cortez + > pfo_cortez.load
#   Both of the above
cat pfo_global.load pfo_cortez.load | loadcomb c > pfo.M2.load

# Load -> Parameter file for volumic strain (v)
cat pfo.M2.load | harprp v > pfo.M2.resp

# Time series of the oceanic load (here get the hourly data of year 1990)
#   -> starts at 1990, day 1 hour 0 minute 0 second 0
#   -> 8766 samples with the sampling period of 3600 seconds.
cat pfo.M2.resp | hartid 1990 1 0 0 0 8766 3600 > pfo.M2.dat
```

To get the load at all frequencies, the script has to be rerun for all the constituents (notice that there is are only few constituents available for the Gulf of California).

Appendix D

BAYTAP

| | |
|-------------|--|
| Function | Tidal analysis |
| License | The program may be freely copied and distributed for academic purposes. Full license of the program is given in the file <code>README.1ST</code> . |
| Source code | Fortran source code provided (compile with <code>-static</code> option) |
| Catalog | Cartwright, Taylor, Edden or Tamura 1987 |
| Pros | Flexible representation of drift, response method for complementary data |
| Cons | No real strain value |

D.1 Input

At least two files are needed by **BAYTAP**: a data file and a parameter file. More data files can be used to account for supplementary data, as barometric pressure.

D.1.1 Data file

They are ASCII files, labeled “INPUTXX.DAT”, where XX is a number between 1 and 99 to be specified in the parameter files (see following section). XX cannot be 05, 06, 16, 30-34.

Two formats are available: the fixed format or the user defined format. We will present only briefly this last format. Excellent documentations and illustrations on the program are available at <http://www.unavco.org:8080/cws/straindata/Notes%20from%202005%20class/>. Only the first 5 lines should have a fixed format:

1. Title of the data set (80 characters)
2. Latitude Longitude Altitude Gravity (4F10)
Latitude and Longitude are in degrees, Altitude in meters and the gravity in cm^2/s (for instance 982.024 as proposed in the documentation, or 0.0, in which case a gravity is automatically computed).
3. Year Month Day Hour (3I5,F10.5)
of the first data sample. Minutes and second are in decimal form (10:30 is 10.5).
4. N_obs Sample_interval Missing_data_flag (I5,F5.0,D15.5)
The sample interval should be given in hours. Be careful of cumulative errors if you had to truncate the sample interval (as for 20 minutes sampling rate= $1/3=0.3333333\dots$) and you

have long time spans.

Any data input larger than the missing data flag will be ignored.

5. Format_of_input_data (80 characters)

A FORTRAN format describing the way the data are written in the file.

Then insert the data as described in Line 5. Here is an example of data file where the data of 1987-Jan-1 12:00 is missing:

```
PFO station - CIB
  33.6092 -116.4553  1200.00    0.000
1987   1   1   0.00000
122737   1   90000.00000
(6F10.2)
-1075.17 -1069.33 -1066.83 -1072.00 -1079.08 -1091.75
-1107.25 -1124.83 -1137.17 -1147.33 -1147.92 99999.99
-1128.33 -1111.83 -1096.58 -1087.17 -1082.42 -1082.50
-1092.42 -1101.33 -1108.58 -1111.92 -1111.50 -1105.75
```

D.1.2 Parameter file

It is an ASCII file, labeled "INTPU05.DAT". Here is an example of the data:

```
&PARAM
SPAN=720
KIND=7
SHIFT=720
DMIN=0.25
LPOUT=0
FILOUT=0
IAUG=1
LAGP=0
LAGINT=0
WEIGHT=1.0
&END
 1987   1   1   0 122737           1
0
   12   1   0
   14   1   0
9999    TITLE
Test CIB BAYTAP
9999
PFO CIB WATER-LEVEL
9999
PFO CIB
VALYDINE GAGE
9999
MH20
BARO ATMOSPHERIC-PRESSURE
```

You can recognize several parts:

1. The parameter part is enclosed between “&PARAM” and “&END” statements. The order of the parameters is not important, but some are necessary:

- **KIND** The tidal constituent to be computed
 - 1 - Gravity tides in μgal . Increase in taken to be positive
 - 2 - North-South tilt, in milliseconds of arc. Tilting down to the north is taken as positive. By setting **AZ** you can compute tilt in a direction **AZ** degrees clockwise from the north.
 - 3 - East-West tilt, in milliseconds of arc. Same as **KIND=2** and **AZ=90**
 - 4 - North-South strain. Positive for an extension. By setting **AZ** you can compute strain in a direction **AZ** degrees clockwise from the north. Units are $\text{nstrain}=10^{-9}$.
 - 5 - East-West strain. Same as **KIND=4** and **AZ=90**
 - 6 - North-West strain. Same as **KIND=4** and **AZ=45**
 - 7 - Strain, or rather the proxy $W/(ga)$, W is the tidal potential, g is the local gravity acceleration and $a = 6371023.6\text{ m}$ the Earth radius. See equations (2.16) and (2.17) to see how to get areal and volumetric strain from it.
 - 8 - Ocean tide in cm. Uplift is positive. It is assumed that the ocean level follows the geoid deformation induced by the tides. In general, it is not true because of additional hydrodynamic effects.
- **SPAN** and **SHIFT**. **SPAN** is the number of data to be processed each time (set by default to 744, which corresponds to 31 days for hourly data) and **SHIFT** is the number of data points the between the first data of each data window consequently analyzed (default is 720). Chances are that the default settings do not fit your study. **SPAN** equals the total length of the data and **SHIFT=0** is a common choice. Hence only one tidal analysis is made for all of the data.
- **IAUG** and the complementary set **LAGP** and **LAGINT**. **IAUG** tells how many data need to be taken into account in the inversion of equation (4.5). **LAGP** is the number K in this equation (default is 0). **LAGINT** is the number K in this equation (default is 0. If **LAGP**>1, put it to 1.)

Some are useful to tune the inversion:

- **DMIN** is the minimal value of D in equation(4.7). Default is 0.25.
- **WEIGHT** is the value of W in equation(4.7). Default is 0.25.
- **MAXITR** The minimal number in the iteration to minimize the ABIC. The default value is 21.
- **IPOTEN** to choose the catalogs (cf. table 2.1). Two choices are available: the Cartwright et al. potential (**IPOTEN=1**)and the Tamura 87 potential (**IPOTEN=2**). Default is 1.
- **LOVNM**. It is not described in the documentation. It seems to switch between two sets of Love numbers.
- **LPOUT** and **FILEOUT**. Set them to 0 if you are only interested in the tidal parameters, and not on derived data (residual, trend). This saves a lot of space.

2. The starting time of the processing, the number of data and the sample interval. The format is (3I5,F5.0,I5,F10.0). The comments are the same as for the data file above.

3. Grouping of tidal constituents

If this number is 0, then the number of group is automatically selected according to the length of the data. Manual setting of the numbers of groups is also possible.

| Duration (days) [grouping=0] | Number of groups | Corresponding manual setting |
|------------------------------|------------------|------------------------------|
| 1-8 | 3 | -2 |
| 8-16 | 5 | -1 |
| 16-180 (6 months) | 12 | 1 |
| 180-364 (6 months-1year) | 14 | 2 |
| 364-2000 (1 year-3 years) | 15 | 3 |
| >2000 (>3 years) | 20 | 4 |
| - | 22 | 5 |
| - | 31 | 6 |

4. Tidal_data_number Data_format Reestimate_step_size_flag

The tidal data are in the file "INPUTXX.DAT" where XX is the tidal data number.

The data format can be fixed (-1 or 0) or user determined (1).

The fixed data format can take into account data gaps. Whether you consider them is given by the "reestimate step size flag". This value is not important for user-defined format.

Repeat this line for supplementary data if needed (IUAG>0).

5. Title, enclosed between two "9999" flags.

6. Station name (40 characters)

7. Instrument name (40 characters). End with "9999".

8. Units of tidal data (40 characters)

9. Title of supplementary data set (40 characters)

One line per supplementary data set.

D.2 Output

The tidal parameters are buried in the middle of the file "OUTPUT06.DAT". Here is an output:

| GROUP | SYMBOL | FACTOR (RMSE) | PHASE (RMSE) (LOCAL, LAG:NEGATIVE) | AMPLITUDE (RMSE) |
|-------|---------------------|--------------------|---------------------------------------|------------------|
| 1 | (1-249 : O1 GROUP) | 0.44629 (0.11352) | 158.050 (14.479) | 6.516 (1.657) |
| 2 | (250-450 : K1 ") | 0.36801 (0.05853) | 177.385 (9.113) | 7.557 (1.202) |
| 3 | (451-655 : M2 ") | 0.52274 (0.01840) | 161.876 (2.025) | 13.934 (0.491) |
| 4 | (656-827 : S2 ") | 1.03225 (0.04498) | 170.803 (2.751) | 12.802 (0.558) |
| 5 | (828-909 : M3 ") | 2.45750 (0.75126) | 22.338 (17.721) | 0.715 (0.218) |

The inversion has been made for 5 groups, named after their major constituents. There are three kind of results: factor, phase and amplitude. In brackets are the error estimation.

The factor and the phase give the response relative to the theoretical tides. They are extracted from the A_m and B_m coefficients of equation (4.6).

The amplitude is a combination of the factor and of the amplitude of the theoretical Earth tides. For instance, although the factor of O_1 is larger than the one of K_1 , the amplitude of the K_1 is larger (see table 2.2 or figure 4.2). **Trust only the waves with the larger amplitudes, since they have larger signal over noise ratio.**

If you made several inversions, the above sequence is repeated several times in the file “OUTPUT06.DAT”.

Bibliography

- D. C. Agnew. SPOTL: Some programs for ocean-tides loading. Technical Report SIO Ref. Ser. 96-8, Scripps Institution of Oceanography, La Jolla, 1996.
- D. C. Agnew. NLOADF: a program for computing ocean-tide loading. *J. Geophys. Res.*, 102: 5109–5110, 1997.
- D.R. Bower. Bedrock fracture parameters from the interpretation of well tides. *J. Geophys. Res.*, 88(B6):5025–5035, 1983.
- B. Buttkus. *Spectral Analysis and Filter Theory in Applied Geophysics*. Springer, 2000.
- R.F. Craig. *Soil Mechanics*. Van Nostrand Reinhold, UK, 4th edition, 1987.
- E. Detournay and A. H.-D. Cheng. Fundamentals of poroelasticity. In J. A. Hudson, editor, *Comprehensive Rock Engineering: Principles, Practice and Projects*, volume 2, pages 113–171, Oxford, UK., 1993. Pergamon Press.
- M.L. Doan. *Étude in-situ des interactions hydromécaniques entre fluides et failles. Application au Laboratoire du Rift de Corinthe*. PhD thesis, Institut de Physique du Globe de Paris, 2005.
- J. E. Elkhoury, E. E. Brodsky, and D. C. Agnew. Seismic waves increase permeability. *Nature*, 441: 1135–1138, 2006.
- W. E. Farrell. Deformation of the earth by surface loads. *Rev. Geophys. Space Phys.*, 10:761–797, 1972.
- J. C. Harrison. Cavity and topographic effects in tilt and strain measurement. *J. Geophys. Res.*, 81 (2):319–328, 1976.
- J. C. Harrison. *Earth Tides*, volume 85 of *Benchmark Papers in Geology*. Van Nostrand Reinhold Company Inc., New York, 1985.
- T. Hartmann and H.-G. Wenzel. The HW95 tidal potential catalog. *Geophys. Res. Lett.*, 22(24): 3553–3556, 1995.
- P.A. Hsieh, J.D. Bredehoeft, and J.M. Farr. Determination of aquifer transmissivity from earth tide analysis. *Water Resour. Res.*, 23(10):1824–1832, 1987.
- R. G. Lyons. *Understanding Digital Signal Processing*. Prentice Hall, Upper Saddle River, NJ, 2nd edition, 2004.

- N. Matsumoto, G. Kitagawa, and E. A. Roeloffs. Hydrologic response to earthquakes in the Haibara well, central Japan: I. Groundwater-level changes revealed using state space decomposition of atmospheric pressure, rainfall, and tidal responses. *Geophys. Jour. Int.*, 2003.
- P. Melchior. *The tides of the planet Earth*. Pergamon Press, Oxford, UK, 2nd edition, 1983.
- E. G. Quilty and E. A. Roeloffs. Removal of barometric pressure response from water level data. *J. Geophys. Res.*, 96(B6):10209–10218, doi=10.1029/91JB00429, 1991.
- R. D. Ray. A global ocean tide model from TOPEX/POSEIDON altimetry: GOT99.2. Technical report, Tech. Memo. NASA/TM-1999-209478, 1999.
- E. A. Roeloffs. Poroelastic techniques in the study of earthquake-related hydrology phenomenon. *Advances in Geophysics*, 37:135–195, 1996.
- H. F. Wang. *Theory of Linear Poroelasticity with Applications to Geomechanics and Hydrogeology*. Princeton Series in Geophysics. Princeton University Press, Princeton, NJ, 2000.
- H. Wilhelm, W. Zürn, and H.-G. Wenzel, editors. *Tidal Phenomena*, volume 66 of *Lecture Notes in Earth Sciences*. Springer, Berlin, Germany, 1997.